

1
2 **Sourcing of Miocene accretionary lapilli on 'Eua, Tonga; atypical dispersal**
3 **distances and tectonic implications for the central Tonga Ridge.**

4
5 **JK Cunningham¹ and AD Beard**

6
7 **Department of Earth and Planetary Sciences, Birkbeck College, University of**
8 **London, Malet Street London WC1E 7HX**

9
10 ¹ Corresponding author, jcunni1248@aol.com, present address: 1 Loudens Close, St
11 Andrews, Fife, Scotland, KY16 9EN, (44) 1344 479348

12
13
14 **Abstract**

15
16 Volcaniclastics hosting accretionary lapilli on the Tonga Ridge were sourced from the
17 remnant Lau Ridge, prior to Lau back-arc basin opening. For the 'Eua occurrences, an
18 atypical dispersal distance of not less than 70 km is estimated, partly arising from the
19 anomalous easterly position of 'Eua. Dispersal within ocean-surface pyroclastic density
20 currents is supported but strike-slip movement in a fault zone south of 'Eua, post
21 Middle Miocene but pre ridge-splitting, can account for part of the dispersal distance by
22 vertical axis block rotation, a tectonic process common on the southern Tonga-
23 Kermadec-Hikurangi trend. In this model, the volcano which sourced the 'Eua tephra
24 was on a subjacent block, rather than the block which hosts 'Eua. After deposition but
25 prior to the opening of the Lau Basin, the accretionary lapilli on 'Eua became displaced
26 by block rotation c. 40 km towards the Tonga trench and away from source.

27
28
29 **Keywords**

30
31 Accretionary lapilli; Tonga Ridge; dispersal distance; block rotation; pyroclastic density
32 currents.

33
34
35 **Introduction**

36
37 Accretionary lapilli are highly ordered types of ash aggregate typically associated with
38 explosive eruptions, where they may form in the plume itself or in pyroclastic density
39 currents as they interact with the co-ignimbrite ash plume. Dispersal may therefore
40 occur subaerially by expansion of the plume, spreading of any atmospheric umbrella
41 cloud, and/or by pyroclastic density currents. The 'Eua accretionary lapilli contain
42 examples typically 10–15 mm in diameter and are accretionary lapilli *sensu stricto*
43 (Brown et al. 2010, Van Eaton & Wilson 2013), as distinguished from less ordered ash
44 pellets and fragile ash aggregates (Brazier et al. 1982; Carey & Sigurdsson 1982;
45 Wiesner et al. 1995; Brown et al. 2012) which rarely survive in that form but are
46 detected in sieve analysis of grain size. Accretionary lapilli have been reported from

47 Miocene volcanoclastics which are exposed on the Nomuka group islands (Ballance et
48 al. 2004) and on 'Eua on the Tonga Ridge (Ballance et al. 2004; Cunningham & Beard
49 2014). The host volcanoclastics were sourced from volcanoes on the Lau Ridge, prior to
50 the splitting of the Lau-Tonga ancestral arc in the latest Late Miocene to form the Lau
51 back-arc basin (Clift et al. 1994, 1995, 1998; Cole et al. 1985; Parson & Wright 1996).
52 Reconstruction of the ancestral ridge places the Nomuka group islands, which are
53 positioned on the west of the Tonga Ridge, at modest dispersal distances from potential
54 source. However, 'Eua is the most easterly of the island exposures along the Tonga
55 Ridge by some margin and this contributes to a dispersal distance from source at the
56 limit of most (but not all) documented occurrences of accretionary lapilli. The
57 resolution of the two problems presented by the anomalous position of 'Eua and the
58 exceptional distance from potential source of the accretionary lapilli found on 'Eua is
59 the focus of this paper. The approach taken to address the two problems is firstly to use
60 data from the Tonga Ridge, the Lau Basin and the Lau Ridge to constrain possible
61 locations for the Middle Miocene source volcano which provided the accretionary lapilli
62 on 'Eua, to consider how the distance between source and destination may have been
63 impacted by post Middle Miocene tectonics, including block rotation, and to estimate
64 the minimum actual contemporary distance from source. Thereafter, the paper
65 examines constraints on possible maximum dispersal distances for the relatively large
66 accretionary lapilli from 'Eua. Discussion is then enabled on whether the anomalous
67 position of 'Eua and the unusual dispersal distance of the 'Eua accretionary lapilli from
68 source can be explained by block rotation within the Tonga microplate and/or a
69 dispersal distance enabled by a pyroclastic density current which traversed the ocean
70 surface before depositing the accretionary lapilli on 'Eua.

71 **Regional setting**

72 Located on the northern part of the Hikurangi-Kermadec-Tonga trend, the Tonga and
73 Lau Ridges are dominantly open marine, as delineated by the 2000 meter contour (Fig.
74 1A). A number of islands occur, some large, but most are barely emergent and
75 exposures are limited. On the Tonga Ridge, the island of 'Eua is an exception, where an
76 uplifted Eocene basement high and overlying sediments are now exposed subaerially.
77 These sediments include deep marine Middle Miocene volcanoclastics. More is known
78 of the Tonga Ridge (Fig. 1B) than the remnant Lau Ridge. Oil industry activity,
79 including 5 exploration wells on Tongatapu, proved that a deep basin of sediment
80 overlays a presumed volcanic arc basement on the north-central part of the Tonga

81 Platform (Cunningham & Anscombe 1985). Scientific cruises (Scholl & Vallier 1985,
82 Stevenson et al. 1994) confirmed this frontal arc basin extended south and established
83 that the present Tonga Ridge is broken into a number of fault-delineated blocks (Fig.
84 1B). On the southern platform, depocentres are identifiable on the west of the basin on
85 isopach A–B (which includes the Miocene), with the sediments thickening generally
86 towards the west. Herzer & Exon (1985) suspected that their alignment along the west
87 side of the basin indicated these sediment "thicks" were fed from volcanic centres
88 "nearby to the west, outside the mapped area". The Lau Ridge bathymetry is very
89 similar to the Tonga Ridge, broadly outlined by the 2000 meter contour (Fig. 1A), but
90 many more islands with a dominantly volcanic aspect dominate the geology (Woodhall
91 1985). Basement rocks are not exposed in the islands, the oldest rocks exposed being
92 Middle Miocene, but volcanism extended from 14.0 to <2.5 Ma, so older geology would
93 have been obscured on volcanic islands. Thus the many Lau Islands which have a long-
94 lived volcanic history provide credible candidates for the volcanic centres "nearby to the
95 west, outside the mapped area" of Herzer & Exon (1985). The island arc andesite
96 character of the Lau Volcanic group (14.0–6.0 Ma) and the age range which includes
97 the Middle Miocene, the age of the mafic volcanoclastics on 'Eua, supports the case. In
98 order to provide a working model for the sourcing of the accretionary lapilli found on
99 the Tonga Ridge, it is now necessary to constrain possible source locations prior to the
100 partition of the ancestral Lau-Tonga Ridge and then consider how the active tectonics in
101 the region may have re-positioned source or settlement site.

102

103 **The accretionary lapilli and the location of possible volcanic sources**

104

105 The reported occurrences of accretionary lapilli on the Tonga Ridge are from Miocene
106 volcanoclastics on 'Eua and on two islands in the Nomuka group (Fig. 1B). The 'Eua
107 occurrences (Fig. 2A–C) range up to 20 mm in maximum dimension and typically occur
108 unsorted in grain to grain contact as thin beds up to 20 cm in thickness. The matrix is
109 coarse-grained (>500 µm) or absent. The 'Eua occurrences exhibit characteristics
110 suggesting they settled to pelagic depths (Ballance et al. 2004; Cunningham & Beard
111 2014) while some of the Nomuka occurrences may have been reworked from the
112 original settlement site (Ballance et al. 2004). The 'Eua host volcanoclastics are typically
113 granulestone/sandstone in grain size, with occasional larger clast sizes, none in excess
114 of 30 mm, and a pelagic planktonic foraminiferal fauna. The fauna are dated at Middle

115 Miocene, c. 14 Ma, with sparse re-worked slightly earlier fauna (Quinterno 1985;
116 Chaproniere 1994), indicating depths of deposition are not less than 1600 meters. A
117 range of sediment gravity flow types (Ballance et al. 2004) are reflected in the host
118 formation, with rare westwards-dipping cross-beds (Fig. 2D). Tappin & Ballance (1994)
119 reported a WNW verging flame structure. In contrast, the 'Eua beds of accretionary
120 lapilli exhibit a narrow size distribution in that they are large, typically 10-15 mm in
121 diameter, and the matrix is fines-depleted or absent. These features are applied to
122 terminal velocity calculations by Cunningham & Beard (2014) to argue that these beds
123 were the result of settling to pelagic depths and were not delivered by sediment gravity
124 flows or submarine pyroclastic flows. The upper size constraint of volcanogenic clasts
125 in the 'Eua volcanoclastics contrasts with the Nomuka host rocks; on Mango in the
126 Nomuka group of islands, Middle (?) Miocene volcanoclastics contain indications of the
127 proximity of volcanic edifices, such as volcanic boulder-bearing debris flow deposits
128 (Ballance et al. 2004). Further south on the T-E block, the detection of volcanic
129 sources is assisted by the availability of close-spaced oil industry data (Gatliff et al.
130 1994). With the high rates of sediment supply implicit in island arc environments, the
131 problem of distinguishing reef structures from buried volcanic edifices is important and
132 has been reviewed (Alexander 1985; Herzer & Exon 1985; Pflueger & Havard 1994;
133 Tappin et al. 1994). Only one volcanic edifice was detected along the Tonga Ridge, in
134 the B-C Late Oligocene to Early Miocene interval and on Block D. No ambiguous
135 structures at all were identified on the T-E block within the interval which includes the
136 Middle Miocene (Gatliff et al. 1994) and "No volcanic structures sourcing unit A-B
137 have yet been identified on the Tonga Ridge" (Tappin et al. 1994). Thus the
138 seismostratigraphy reveals no obvious local source on the Tonga Ridge for the
139 accretionary lapilli, either for the Nomuka group or the 'Eua occurrences. The regional
140 setting suggests that sources would be to the west and on the remnant Lau Ridge, where
141 long-lived volcanic islands exist.

142 **Tectonics**

143 The study area of the SW Pacific is a tectonic province with a relatively well-
144 documented geological history, particularly with respect to back-arc extension/basin
145 formation processes (Packham 1978; Tappin 1993; Sager et al. 1994; Tappin et al.
146 1994; Parson and Wright 1996; Taylor et al. 1996). In the south of the region, on the
147 Tonga-Kermadec-Hikurangi trend, subducting oceanic plate encounters continental
148 crust on South Island, New Zealand (Lamb 2011). Further north, the environment is

149 oceanic. A more sophisticated model for Lau Basin formation (Figs. 3A, 3C) replaced a
150 simple mid-oceanic type spreading centre model with a two-phase model (Parson et al.
151 1994; Parson & Wright 1996; Taylor et al. 1996). The Lau basin floor geology is
152 asymmetric; patterns of strong positive magnetic intensity are exhibited east of a line
153 running NNW across the Lau Basin at roughly 317° , reflecting the new oceanic crust
154 being created at the Central and Eastern Lau spreading centres. However, west of that
155 line and east of the 2000 meter isobath on the Lau Ridge, an irregular terrain of north-
156 trending horst/grabens occurs where specific magnetization events were not well
157 delineated, attributed to diffuse spreading to form “extended arc crust”. In broad terms,
158 the ancestral Lau/Tonga Ridge arc crust split and experienced extension to the east of
159 the active arc volcanoes on the remnant Lau Ridge by:

- 160 • graben/half-graben faulting accompanied by intrusive activity which mark the
161 location of repeated “failed” spreading centres (creating the “extended arc
162 crust”), before:
- 163 • formation of new crust occurred continuously at more typical mid-ocean ridge
164 type spreading centres (the Central Lau Spreading Centre/East Lau Spreading
165 Centre , which were initiated in the north of the Lau Basin and propagated
166 southwards.

167 During these processes, Lau Ridge and intra-basin volcanism occurred and eventually
168 ceased, before restoration of back-arc volcanism on the currently active Tofua Arc. The
169 net effect is that of an apparent rotation of the Tonga Ridge, the current active arc, some
170 20° clockwise, away from the remnant Lau Ridge segment of the ancestral arc. With no
171 compelling evidence to support a source on the Tonga Ridge, 'Eua appears to be at a
172 considerable distance from a source which must have existed further to the west on the
173 ancestral Lau-Tonga ridge. Using present sea-bed depth contours at 1000 and 2000
174 meters to estimate the width of the ancestral arc elements, an outline reconstruction
175 (Fig. 3B) is achieved by rotating the Tonga Ridge in the horizontal plane back to the
176 west by the c. 20° estimated by Sager et al. (1994). On Block T–E, the distance
177 between the western edge of the Tonga Ridge and 'Eua, where it thins against the proto-
178 'Eua submergent high is c. 61 km (Fig. 3A), before correction for extension due to
179 post-Middle Miocene faulting. Post-Middle Miocene sub-vertical fault patterns on the
180 Tonga Ridge segment do not suggest this will be material, when compared with pre-
181 Middle Miocene graben/half graben faulting which may be listric at depth. However,
182 the threat of underestimation of extension due to unidentified small faults (Twiss &

183 Moores 2007), supports the application of a non-trivial provision, say 10%, which
184 would bring the 61 km estimate down to c. 55 km pre-fault extension. The Tonga
185 frontal arc basin segment terminates abruptly on the west with down-to-Tofua faulting
186 (Herzer & Exon 1985). The footprint of any volcanic source on the remnant Lau Ridge
187 segment requires estimation. The profile of the currently active Tofua arc volcanoes
188 provide possible analogues of Lau Ridge volcanic sources. At base, these range up to c.
189 30 km in width, excluding composite structures which are wider (Chase 1985, Fig. 1).
190 On this basis, 55 plus 15 km = 70 km is indicative of the minimum distance from a
191 source on the eastern edge of the remnant Lau Ridge segment. If the source volcano
192 was originally in what is now the extended arc crust of the western Lau Basin, this
193 figure is increased, but no data is available from the ODP sites in the Lau Basin to
194 constrain this possibility, as none of these reached the Middle Miocene (Fig. 3A). A
195 much higher figure is required if a structure in the position of Ono-i-Lau is considered.
196 In the Lau Basin at the longitude under study, c.105 km of extended arc crust exists and
197 the distance from Ono-i-Lau to the eastern edge of the Lau Ridge is 75 km.
198 The more local effects of individual block rotation are now considered. During re-
199 processing of oil industry data on the T-E Block, it was noted that a number of
200 physiographic features of the block would be explained if it had rotated 30⁰
201 anticlockwise (Gatliff et al. 1994). One feature is the atypical triangular shape of the
202 Tongatapu-‘Eua block as a whole (Fig. 1B), as reflected at the 1000 m isobath. ‘Eua is
203 closer to the eastern margin of the frontal arc basin than any other basement high, and as
204 an emergent island with an elevation of 912 meters, is much higher. To further explore
205 whether there is seismostratigraphic/geophysical support for the rotation proposition, a
206 number of sources of data were superimposed on Blocks A, B and T-E (Fig. 4). There
207 are clearly a number of departures from the Tonga Ridge NNE-SSW ridge-parallel
208 structural trend, localised to the southern margin of Block T-E. On Block T-E, a trend
209 in total magnetic intensity highs, broadly coincident with basement highs (Gatliff et al.
210 1994) departs from trend and is deflected east of ‘Eua. Further south, on Blocks A and
211 B, a trend of magnetic intensity anomalies (Stevenson & Childs 1985), coincident with
212 ridge-parallel gravity/basement highs, is abruptly curtailed as the southern margin of the
213 T-E block is encountered. The 'Eua Channel Fault, a major structural feature on the
214 southern Tonga Ridge, disappears north of the Block T-E southern margin, where the
215 Tongatapu/‘Eua Channel depocentre was identified (Herzer and Exon 1985, Gatliff et
216 al. 1994).

217 The three total magnetic intensity highs immediately east of 'Eua on the Tongatapu-
218 'Eua block appear to be displaced by a strike-slip fault c. 40 km to the east of the trend
219 of the magnetic intensity anomalies on Blocks A and B. This would have the effect of
220 anticlockwise rotation *sensu* Gatliff et al. (1994). Further south on the Tonga-
221 Kermadec-Hikurangi trend, Lamb (2011) reviews the tectonics and kinetics of faulting
222 in the leading Australian plate continental crust, which accommodates the effects of
223 non-orthogonal subduction. The distinctive faulting styles described include those
224 which could explain features on the T–E block (Cunningham & Anscombe 1985, Fig. 2)
225 by inverting the rotation effect of strike slip faulting on arcuate faults (Lamb 2011, Fig.
226 18 a), combined with dextral strike slip faulting on a curved strike slip fault “hinge”
227 (Lamb 2011, Fig. 18 f). Block rotation may be contemporaneous with or post-date
228 block formation. Block formation by ridge-traverse faults may have begun “long before
229 the block geometry became so prominent after Late Miocene time” (Scholl & Herzer
230 1994). Since the western margin of the T–E block has a down-to-Tofua NNE-SSW fault
231 pattern consistent with the other blocks, any rotation, as noted by Gatliff et al. (1994),
232 must have occurred before the ancestral Lau Tonga arc splitting commenced in the late
233 Late Miocene (5.3 Ma). An event at c. 10 Ma was detected by sediment backstripping
234 analysis on the Tonga Ridge at ODP 841 (Clift et al. 1994) and hence in the early Late
235 Miocene. We now propose a model by which block rotation may have contributed
236 towards the dispersal distance anomaly. The model crucially suggests that, pre-ancestral
237 Lau-Tonga Ridge splitting, a Middle Miocene volcano on what would become
238 subjacent Block A sourced the 'Eua accretionary lapilli found on what would become
239 Block T–E. Anticlockwise block rotation after deposition, but before Lau Basin opening
240 commenced in the late Late Miocene, affects Block T–E, but not A or N. After rotation
241 of this block, the Nomuka Group islands maintain their distance from source volcano,
242 but 'Eua has been displaced tectonically 40 km eastwards from the tephra source. The
243 distance between source and resting place for the accretionary lapilli has been increased
244 by 40 km even before ridge splitting in the latest Late Miocene carries 'Eua further east.

245

246 **Constraining dispersal distances for accretionary lapilli**

247 The evidence for final deposition of the 'Eua accretionary lapilli by settling through a
248 marine column of not less than 1600 meters, as presented in Cunningham & Beard
249 (2014), has been summarised earlier. The processes by which they could have reached
250 the point of settlement will now be reviewed. The present Tofua active volcanic arc

(Fig. 1B) is composed of emergent, barely emergent and submarine volcanic edifices at modest depths and may be a good proxy for the Middle Miocene ancestral active volcanic arc, given the dominantly volcanic insular geology as described earlier for the remnant Lau Ridge. The ash clouds within which ash aggregates form (Brown et al. 2012) are typically associated with subaerial explosive volcanic eruptions, although shallow marine eruptions can also be contenders if they breach water depths (McBirney 1963; Wright & Gamble 1999; White et al. 2003) with the creation of an atmospheric ash cloud. The 'Eua accretionary lapilli may therefore have formed during an explosive volcanic eruption initiated subaerially from an emergent volcanic edifice or at shallow depths. In addition, proximity of the ocean surface permits the possibility of formation of accretionary lapilli in secondary ash-rich steam clouds as pyroclastic density currents enter the sea (Dufek et al. 2007). Dispersal may take place subaerially within the eruption plume/umbrella cloud or as pyroclastic density currents travel across the sea surface (Allen & Cas 2001; Carey et al. 1996; Maeno & Taniguchi 2007). The substantial distances by which less-ordered ash aggregates can be dispersed from source subaerially are well established; ash aggregates dispersed in the eruption plume at Mt St Helens were detected at 200 km from source (Carey & Sigurdsson 1982). In contrast, the dispersal of relatively large and dense accretionary lapilli within the eruption plume must be restricted by their significant mass to more modest dispersal distances from the source volcano, as constrained in tephra dispersal models (Walker et al. 1971; Walker 1981; Carey & Sparks 1986; Pfeiffer et al. 2005; Folch 2012). Accretionary lapilli are technically lapilli, falling within the 2–64 mm range, (Schmid 1981; Fisher & Schmincke 1984). Lapilli-sized tephra can be dense juvenile/country rock clasts, mafic scoria or vesicular silicic pumice clasts. Reported specific gravities of accretionary lapilli, which are dominantly silicic, are in the range of 1200–1500 kg m⁻³ (Sparks et al. 1997). The 'Eua examples are mafic in composition and should therefore be at the upper end of this spectrum or slightly exceed it. Isopleths for 16 mm-sized lapilli for known eruptions show maximum dispersal distance in the range of 20–30 km (Carey & Sparks 1986), for tephra at density of 2500 kg m⁻³ and “larger centrimetric and millimetric fragments typically settle in minutes to few hours at distances of the order of tens of km from the volcano” (Folch 2012). Grain size directly influences terminal velocity of descent of a particle. This varies significantly with height in the atmosphere and departure from sphericity (Dellino et al. 2005). These parameters are accommodated in most tephra transport and dispersal models. Table 1 provides indicative terminal

285 velocities over a range of heights (Pfeiffer et al. 2005) for particles of $\Phi = -4$ (=16
286 mm), density of 1500 kg m^{-3} , and departure from sphericity. These particles are close to
287 the typical size of the 'Eua accretionary lapilli. The density of 1500 kg m^{-3} is
288 appropriate, as discussed earlier (advanced palagonitisation obscures the original
289 density of the constituent glass particles). These figures would underestimate terminal
290 velocity for the notably spheroidal 'Eua accretionary lapilli. The range of contemporary
291 prevailing wind speeds in the Lesser Antilles range from 5.55 m sec^{-1} in the stratosphere
292 and up to 25 m sec^{-1} in the upper troposphere (Sigurdsson et al. 1980). Based on input of
293 the 16 mm clast isopleth for Cotopaxi layer 3, Burden et al. (2011) estimate plume
294 height between 26 km and 32.5 km with a wind speed of 35 m sec^{-1} . If these wind
295 speeds were applicable to the SW Pacific in the Middle Miocene, the effects of wind
296 advection should be modest for tephra the size of the 'Eua accretionary lapilli.
297 Complexity is introduced by the formation of aggregates during plume development,
298 whether in the form of accretionary lapilli or less-ordered ash aggregates, as this is
299 complex to model (Costa et al. 2010); accretionary lapilli often occur in
300 phreatomagmatic eruptions, where phase changes involving latent heat release might
301 increment the upwards convection vector and counter the dominant role, in most
302 models, of the downward terminal ("settling") velocity of descent. Modelling of the
303 phreatomagmatic 25.4 ka Oruanui event (Van Eaton et al. 2012), an ultra-Plinian event,
304 instead of a simple plume/high level umbrella cloud with lower level co-ignimbrite ash
305 clouds, produced "hybrid" ash clouds generated both from the plume and from buoyant
306 co-ignimbrite ash clouds which rise to plume heights. Concentrically layered
307 accretionary lapilli similar to those in 'Eua were dispersed at distances of 120 km from
308 source (Van Eaton & Wilson 2013) in this event. The 25.4 ka Oruanui event is
309 statistically unusual; only 156 (2.3 %) such events are reported from a total of 6736 in
310 the Smithsonian Institute database (Siebert and Simkin 2002–2014). Occurrences from
311 more modest events are reported from dispersal within the Soufriere St Vincent plume
312 at 36 km from source (Brazier et al. 1982) and dispersed within pyroclastic density
313 currents at Mt St Helens at c. 25 km (Fisher et al. 1987), and these are closer to ash
314 pellets as defined (Brown et al 2010; Van Eaton & Wilson 2013), rather than
315 accretionary lapilli. Surface dispersal over the ocean surface is now considered.
316 Pyroclastic density currents can partition into a coarse, dense-clast rich submarine flow
317 and a dilute pyroclastic surface flow running at the surface on entering the sea, as seen
318 with experiments and simulations referred to observed/inferred events and their deposits

319 (Freundt 2003; Trofimovs et al. 2006; Dufek & Bergantz 2007; Trofimovs et al. 2008;
320 Dufek et al. 2009). Observations of the deposits of the Kos Plateau Tuff (Allen & Cas
321 2001) supported this model, with the loss of the coarsest vent and conduit-derived lithic
322 clasts over the sea due to sinking, while over land, saltation was considered to have
323 preserved the coarser element in the resulting ignimbrites. Saltation may also occur over
324 water and be accentuated by the occurrence of pumice rafts (Fiske et al. 2001) while,
325 conversely, transport capacity will be influenced by areal dilution, as momentum
326 transfer between large and small particles is diminished (Dufek & Bergantz 2007;
327 Dufek et al. 2009). Such surface flows have travelled for considerable distances (Table
328 2), carrying bomb and lapilli-sized clasts, in addition to ash and hot gas. In conclusion,
329 for plume/umbrella cloud dispersal within the atmosphere, the "tens of km" metric is
330 supported. For pyroclastic density current-enabled dispersal over land, only a
331 statistically unlikely ultra-Plinian event is capable of providing dispersal via the
332 atmosphere for the minimum 70 km dispersal scenario, (considering the source was
333 close to the eastern edge of the remnant Lau Ridge segment). In contrast, for
334 pyroclastic density current-enabled dispersal across the ocean surface, there is some
335 evidence that relatively modest magnitude events could provide dispersal distances
336 which contribute significantly to the scenario.

337 **Discussion and conclusions**

338 The accretionary lapilli on 'Eua, Tonga, occur in Middle Miocene pelagic volcanoclastic
339 sediments with no evidence for a proximal volcanic source. A contemporary distance
340 which is unlikely to be less than 70 km, and may be much more, from a source on the
341 Lau segment of the ancestral Lau-Tonga Ridge, is estimated from seismostratigraphic
342 and other data. This is much farther than would be expected for dispersal of these
343 spheroids of significant mass, unless an exceptional ultra-Plinian source is invoked.
344 Tephra fall associated with an ultra-Plinian event on the scale of the Oruanui at 25.4 ka
345 (Van Eaton & Wilson 2013) could, *prima facie*, resolve the dispersal distance problem,
346 since the dispersal distances of accretionary lapilli in the atmosphere by the eruption
347 plume and pyroclastic density currents in that event were substantial. However, there is
348 no field evidence in the area under study for an ultra-Plinian event in the Middle
349 Miocene. At 530 km³ DRE, the Oruanui event is exceptional and unit 8, which contains
350 the highly dispersed occurrences, exhibits characteristics which suggest that the
351 eruption produced an extremely high mass eruption rate ($\geq 10^9$ kg s⁻¹), with numerical
352 simulations (Van Eaton et al. 2012) implying the potential for transportation of tephra to

353 stratospheric heights. Explosive volcanic events of a much more modest magnitude, but
354 driving pyroclastic density currents over the ocean surface, have dispersed tephra to
355 considerable distances (Table 2), with larger tephra being carried as far as 65 km. The
356 restriction of upper size carried, depending on mass flux during the event, has
357 significance for the Tongan insular Miocene, where the absence of clasts exceeding 30
358 mm has been attributed to some trapping mechanism elsewhere (Ballance et al. 2004)
359 for clasts of greater size. Delivery by sediment gravity flows is probable for most of the
360 volcanoclastics on the 'Eua high (Tappin & Ballance 1994; Ballance et al. 2004).
361 However, for any component of the 'Eua volcanoclastics delivered by ocean surface
362 pyroclastic density currents, an alternative process by which upper grain size is restricted
363 is suggested. Furthermore, the rare westwards-dipping cross-beds in the 'Eua
364 volcanoclastics (Fig. 2D) may be attributable to sediment overloading on the 'Eua high
365 by periodic ocean surface pyroclastic density currents and consequential westwards
366 backflow.

367 While delivery by pyroclastic density current over the ocean surface may explain all or
368 part of the dispersal distance issue, it does not explain the anomalous position of the
369 'Eua high; 'Eua is positioned much further from the western edge of the Tonga Ridge
370 than any other island. The discontinuities in trends at the southern Block T–E margin,
371 interpreted as block rotation of a particular type, provides a tectonic explanation for this
372 anomaly. The relative thickness of sediment in the Tongatapu/'Eua Channel depocentre
373 (Fig. 4) fits well within this model: with block rotation occurring in the Late Miocene,
374 but pre-splitting, the Tongatapu-'Eua Channel basin would have been 40 km closer to
375 the source volcanoes to the west for part of the interval 14 – 5.3 Ma, thus only 30 km
376 from source on the minimum 70 km scenario.

377 For the rotation event to have contributed 40 km to the 'Eua accretionary lapilli
378 dispersal distance, a number of conditions must apply. Firstly it must pre-date splitting
379 of the ancestral Lau/Tonga Ridge which commenced in latest Late Miocene (5.3 Ma),
380 secondly post-date the deposition of the accretionary lapilli on proto-'Eua at 14 Ma, and
381 thirdly, the accretionary lapilli must have been sourced from a volcano on the ancestral
382 Lau-Tonga Ridge segment which became Block A.

383 We favour a model where the accretionary lapilli on 'Eua finally settled through a
384 marine column of not less than 1600 meters. Their delivery to the final resting site was
385 most likely achieved by transport within a pyroclastic density current travelling over the
386 ocean surface which, even in the case of those initiated by small/moderate explosive

387 volcanic events, have delivered relatively large tephra considerable distances from
388 source. A dual model, comprising block rotation and dispersal by ocean surface
389 pyroclastic density currents, can explain the anomalies described and accommodate a
390 large range of possible dispersal distances from a source of modest magnitude. The
391 dating of block formation and of subsequent movement is however problematic; ridge-
392 normal faulting is only strongly expressed in displacement of the A–B isopach,
393 implying that it postdated late Late Miocene. Only detailed palaeomagnetic studies of
394 the host Middle Miocene volcanoclastics on ‘Eua could increase precision in this regard;
395 the ubiquity of magnetite in thin hemipelagites which occur in these rocks would make
396 such studies worthwhile.

397

398 **Acknowledgements**

399

400 JKC acknowledges the many in Tonga and on ‘Eua who assisted during 2 years spent
401 there and during more recent visits. Funding from the UK Overseas Development
402 Agency and Birkbeck College supported the fieldwork. Shell International kindly
403 provided copies of data sheets and their final report. Discussion, help and
404 encouragement from Peter Ballance was crucial in framing the objectives of this paper.
405 Subsequent assistance from Rick Hoblitt, Sharon Allen, Ben Ellis and Alexa Van Eaton
406 greatly improved the execution. The detailed review points of Martin Jutzeler and an
407 anonymous reviewer were crucial in achieving the final draft. The editors are thanked
408 for their support.

409

410

411

412

413

414

415 **References**

416

417 Alexander, C 1985. 2-D gravity and magnetic modelling of subsurface domical
418 structure 11/14: Volcanic episodes in 'Eua, Tonga. In: Scholl DW, Vallier TL eds.
419 Geology and Offshore Resources of Pacific Island Arcs–Tonga Region. Earth Science
420 Series 2. Houston, Texas, Circum-Pacific Council for Energy and Mineral Resources.
421 Pp. 197–202.

422

423 Allen SR, Cas RAF 2001. Transport of pyroclastic flows across the sea during the
424 explosive rhyolitic eruption of the Kos Plateau Tuff, Greece. *Bulletin of Volcanology*
425 62(6–7): 441–456.

426

427 Austin J, Taylor FW, Cagle CD 1989. Seismic stratigraphy of the central Tonga Ridge.
428 *Marine and Petroleum Geology* 6: 71–92.

429

430 Ballance PF, Tappin DR, Wilkinson IP 2004. Volcaniclastic gravity flow sedimentation
431 on a frontal arc platform: the Miocene of Tonga. *New Zealand Journal of Geology and*
432 *Geophysics* 47: 567–587.

- 433
434 Brazier S, Davis AN, Sigurdsson H, Sparks RSJ 1982. Fall-out and deposition of
435 volcanic ash during the 1979 explosive eruption of the Soufriere of St. Vincent. *Journal*
436 *of Volcanology and Geothermal Research* 14: 335–359.
437
- 438 Brown RJ, Branney MJ, Maher C, Harris PD 2010. Origin of accretionary lapilli within
439 ground-hugging density currents: evidence from pyroclastic couplets on Tenerife.
440 *Bulletin of the Geological Society of America* 122: 305–320.
441
- 442 Brown RJ, Bonadonna C, Durant AJ 2012. A review of volcanic ash aggregation.
443 *Physics and Chemistry of the Earth* 45–46: 65–78.
444
- 445 Burden RE, Phillips JC, Hincks TK 2011. Estimating volcanic plume heights from
446 depositional clast size. *Journal of Geophysical Research* 116: B11206.
447 doi:10.1029/2011JB008548.
448
- 449 Carey SN, Sigurdsson H 1982. Influence of particle aggregation on deposition of
450 distal tephra from the May 18, 1980, eruption of Mount St. Helens volcano. *Journal of*
451 *Geophysical Research* 87: 7061–7072.
452
- 453 Carey SN, Sparks RSJ 1986. Quantitative models of the fallout and dispersal of tephra
454 from volcanic eruption columns. *Bulletin of Volcanology* 48: 109–125.
455
- 456 Carey SN, Sigurdsson H, Mandeville C, Bronto S 1996. Pyroclastic flows and surges
457 over water: an example from the 1883 Krakatau eruption. *Bulletin of Volcanology* 57:
458 493–511.
459
- 460 Chaproniere GCH 1994. Middle and Late Eocene, Neogene, and Quaternary
461 foraminiferal faunas from 'Eua and Vava'u Islands, Tonga group, In: Stevenson AJ,
462 Herzer RH, Ballance PF eds. *Geology and Submarine Resources of the Tonga-Lau-Fiji*
463 *Region. SOPAC Technical Bulletin* 8. Suva, Fiji, South Pacific Applied Geoscience
464 Commission. Pp. 21–44.
465
- 466 Chase TE 1985. Submarine topography of the Tonga-Fiji Region and the southern
467 Tonga platform area. In: Scholl DW, Vallier TL eds. *Geology and Offshore Resources*
468 *of Pacific Island Arcs–Tonga Region. Earth Science Series* 2. Houston, Texas, Circum-
469 Pacific Council for Energy and Mineral Resources. Pp. 21.
470
- 471 Clift PD, Bednarz UB, Bøe R, et al. 1994. Sedimentation on the Tonga forearc related
472 to arc rifting, subduction erosion, and ridge collision: a synthesis of results from sites
473 840 and 841. In: Hawkins JW, Parson LM, Allan JF eds. *Proceedings of the Ocean*
474 *Drilling Program, Scientific Results, Vol. 135.* College Station, Texas. Pp. 843–873.
475
- 476 Clift PD and ODP Leg 135 Scientific Party 1995. Volcanism and sedimentation in a
477 rifting island arc terrain: an example from Tonga, SW Pacific. In: Smellie JL ed.
478 *Volcanism associated with extension at consuming plate margins.* Geological Society of
479 London, Special Publication 88. Pp. 29–52.
480
- 481 Clift PD, McCleod CJ, Tappin DR, Wright DJ, Bloomer SH 1998. Tectonic controls on
482 sedimentation and diagenesis in the Tonga Trench and forearc, southwest Pacific.
483 *Geological Society of America Bulletin* 110: 483–496.

- 484
485 Cole JW, Gill JB, Woodhall D 1985. Petrological history of the Lau Ridge, Fiji. In:
486 Scholl DW, Vallier TL eds. *Geology and Offshore Resources of Pacific Island Arcs–*
487 *Tonga Region. Earth Science Series 2.* Houston, Texas, Circum-Pacific Council for
488 Energy and Mineral Resources. Pp. 379–391.
489
490 Costa A, Folch A, Macedonio G, Durant A. 2010. Modelling transport and aggregation
491 of volcanic ash particles. EGU General Assembly 2–7 May 2010, Vienna, Austria.
492 8965.
493
494 Cunningham JK, Anscombe KJ 1985. Geology of 'Eua and other islands, Kingdom of
495 Tonga. In: Scholl DW, Vallier TL eds. *Geology and Offshore Resources of Pacific*
496 *Island Arcs–Tonga Region. Earth Science Series 2.* Houston, Texas, Circum-Pacific
497 Council for Energy and Mineral Resources. Pp. 221–257.
498
499 Cunningham JK, Beard AD 2014. An unusual occurrence of mafic accretionary lapilli
500 in deep-marine volcanoclastics on 'Eua, Tonga: palaeoenvironment and process. *Journal*
501 *of Volcanology and Geothermal Research* 274: 139–151.
502
503 Dellino P, Mele D, Bonasia R, Braia G, La Volpe L, Sulpizio R 2005. The analysis of the
504 influence of pumice shape on its terminal velocity. *Geophysical Research Letters*, 32:
505 L21306. doi:10.1029/2005GL023954.
506
507 Dufek J, Bergantz GW 2007. Dynamics and deposits generated by the Kos Plateau Tuff
508 eruption: Controls of basal particle loss on pyroclastic flow transport. *Geochemistry*
509 *Geophysics Geosystems* 8, Q12. doi:10.1029/2007GC001741.
510
511 Dufek J, Manga M, Staedter M 2007. Littoral blasts: Pumice-water heat transfer and
512 the conditions for steam explosions when pyroclastic flows enter the ocean. *Journal of*
513 *Geophysical Research* 112, B11201. doi:10.1029/2006JB004910.
514
515 Dufek J, Wexler J, Manga M 2009. Transport capacity of pyroclastic density currents:
516 Experiments and models of substrate-flow interaction. *Journal of Geophysical Research*
517 114: B11203. doi:10.1029/2008JB006216.
518
519 Fisher RV, Glicken H, Hoblitt RP 1987. May 18, 1980, Mount St. Helens Deposits in
520 South Coldwater Creek, Washington. *Journal of Geophysical Research - Solid Earth* 92
521 (B10): 10267–10283.
522
523 Fisher RV, Schmincke H-U 1984. *Pyroclastic rocks.* Berlin, Springer-Verlag. 472 p.
524
525 Fiske RS, Cashman, KV, Shibata, A, Watanabe K 1998. Tephra dispersal from
526 Myojinsho, Japan, during its shallow submarine eruption of 1952–1953: *Bulletin of*
527 *Volcanology* 59: 262–275.
528
529 Folch A 2012. A review of tephra transport and dispersal models: Evolution, current
530 status, and future perspectives. *Journal of Volcanology and Geothermal Research* 235–
531 236: 96–115.
532
533 Freundt A 2003. Entrance of hot pyroclastic flows into the sea: experimental
534 observations. *Bulletin of Volcanology* 65: 144–164. doi: 10.1007/s00445–002–0250–1.
535

- 536 Gatliff RW, Pflueger JC, Havard KR, Helu SP 1994. Structure, seismic stratigraphy and
537 petroleum potential of the Tongatapu -'Eua area of the Kingdom of Tonga. In:
538 Stevenson AJ, Herzer RH, Ballance PF eds. Geology and Submarine Resources of the
539 Tonga-Lau-Fiji Region. SOPAC Technical Bulletin 8. Suva, Fiji, South Pacific Applied
540 Geoscience Commission. Pp. 107–119.
541
- 542 Herzer RH, Exon NF 1985. Structure and basin analysis of the southern Tonga forearc.
543 In: Scholl DW, Vallier TL eds. Geology and Offshore Resources of Pacific Island Arcs–
544 Tonga Region. Earth Science Series 2. Houston, Texas, Circum-Pacific Council for
545 Energy and Mineral Resources. Pp. 55–74.
546
- 547 IAGA Division 1 Study Group 1976. International geomagnetic reference field 1965.
548 Journal of Geophysical Research 74: 4407–4408.
549
- 550 Lamb S 2011. Cenozoic tectonic evolution of the New Zealand plate-boundary zone: A
551 paleomagnetic perspective. Tectonophysics 509: 135–164.
552
- 553 Maeno F, Taniguchi H 2007. Spatiotemporal evolution of a marine caldera-forming
554 eruption, generating a low-aspect ratio pyroclastic flow, 7.3 ka, Kikai caldera,
555 Japan: Implication from near-vent eruptive deposits. Journal of Volcanology and
556 Geothermal Research 167: 212–238.
557
- 558 McBirney AR 1963. Factors governing the nature of submarine volcanism. Bulletin of
559 Volcanology 26 (Pt. 2): 455–469.
560
- 561 Packham, G.H 1978. Evolution of a simple island arc: The Lau-Tonga Ridge. Bulletin
562 of the Australian Society of Exploration Geophysicists 9: 133–140.
563
- 564 Parson LM, Rothwell RG, MacLeod CJ 1994. Tectonics and sedimentation in the Lau
565 Basin (southwest Pacific). In: Hawkins JW, Parson LM, Allan JF eds. Proceedings of the
566 Ocean Drilling Program, Scientific Results, Vol. 135. College Station, Texas. Pp. 9–22.
567
- 568 Parson LM, Wright IC 1996. The Lau-Havre-Taupo back-arc basin: A
569 southward-propagating, multi-stage evolution from rifting to spreading.
570 Tectonophysics 263: 1–22.
571
- 572 Pfeiffer T, Costa A, Macedonio G 2005. A model for the numerical simulation of
573 tephra deposits. Journal of Volcanology and Geothermal Research 140: 273–294.
574
- 575 Pflueger JC, Havard KR 1994. A re-examination of the line 11/14 anomaly on the
576 Southern Tonga Platform. In: Stevenson AJ, Herzer RH, Ballance PF eds. Geology and
577 Submarine Resources of the Tonga-Lau-Fiji Region. SOPAC Technical Bulletin 8.
578 Suva, Fiji, South Pacific Applied Geoscience Commission. Pp. 107–119.
579
- 580 Quinterno PJ 1985. Cenozoic planktonic foraminifers and coccoliths from 'Eua,
581 Tongatapu and Nomuka Islands, southwest Pacific Ocean. In: Scholl DW, Vallier TL
582 eds. Geology and Offshore Resources of Pacific Island Arcs–Tonga Region. Earth
583 Science Series 2. Houston, Texas, Circum-Pacific Council for Energy and Mineral
584 Resources. Pp. 259–267.
585

- 586 Sager WW, MacLeod CJ, Abrahamsen N 1994. Palaeomagnetic constraints on Tonga
587 Arc tectonic rotation from sediments drilled at Sites 840 and 841. In: Hawkins JW,
588 Parson LM, Allan JF eds. Proceedings of the Ocean Drilling Program, Scientific
589 Results, Vol. 135. College Station, Texas. Pp.763–783.
590
- 591 Schmid R 1981. Descriptive nomenclature and classification of pyroclastic deposits and
592 fragments: Recommendations of the International Union of Geological Sciences
593 Subcommittee on the Systematics of Igneous Rocks. The Geological Society of
594 America, Boulder, Colorado. Volume 9. Pp. 41–43.
595
- 596 Scholl DW, Vallier TL eds. 1985. Geology and offshore resources of the Pacific island
597 arcs–Tonga region. Earth Science Series 2. Houston, Texas, Circum-Pacific Council for
598 Energy and Mineral Resources. 488 p.
599
- 600 Scholl DW, Herzer RH 1994. Geology and resource potential of the southern Tonga–
601 Lau region. In: Stevenson AJ, Herzer RH, Ballance PF eds. Geology and Submarine
602 Resources of the Tonga-Lau-Fiji Region. SOPAC Technical Bulletin 8. Suva, Fiji,
603 South Pacific Applied Geoscience Commission. Pp. 329–335.
604
- 605 Siebert L, Simkin T 2002–2014. Volcanoes of the World: an Illustrated Catalog of
606 Holocene Volcanoes and their Eruptions. Smithsonian Institution, Global Volcanism
607 Program Digital Information Series, GVP–3,
608 (<http://www.volcano.si.edu/world/> accessed 12th December 2014).
609
- 610 Sigurdsson H, Sparks RSJ, Carey SN, Huang TC 1980. Volcanogenic sedimentation in
611 the Lesser Antilles Arc. The Journal of Geology 88(5): 523–540.
612
- 613 Sparks RSJ, Bursik MI, Carey SN, Gilbert JE, Glaze L, Sigurdsson, H, Woods AW
614 1997. Particle aggregation in plumes, In: Volcanic Plumes. England, John Wiley &
615 Sons. Pp. 431–462.
616
- 617 Stevenson AJ, Childs JR 1985. Single channel seismic and geopotential data collection
618 and processing. In: Scholl DW, Vallier TL eds. Geology and Offshore Resources of
619 Pacific Island Arcs–Tonga Region. Earth Science Series 2. Houston, Texas, Circum-
620 Pacific Council for Energy and Mineral Resources. Pp. 27–29.
621
- 622 Stevenson AJ, Herzer RH, Ballance PF 1994. Geology and submarine resources of the
623 Tonga-Lau-Fiji region. SOPAC Technical Bulletin 8. Suva, Fiji, South Pacific Applied
624 Geoscience Commission. 350 p.
625
- 626 Tappin DR 1993. The Tonga Frontal Arc Basin. In: Ballance PF, ed. South Pacific
627 Sedimentary Basins. Sedimentary Basins of the World 2. Elsevier. Pp. 157–176.
628
- 629 Tappin DR, Ballance PF 1994. Contributions to the sedimentary geology of 'Eua Island,
630 Kingdom of Tonga: reworking in an oceanic forearc. In: Stevenson AJ, Herzer RH,
631 Ballance PF eds. Geology and Submarine Resources of the Tonga-Lau-Fiji Region.
632 SOPAC Technical Bulletin 8. Suva, Fiji, South Pacific Applied Geoscience
633 Commission. Pp.1–20.
634
- 635 Tappin DR, Herzer RH, Stevenson AJ 1994. Structure and history of an oceanic
636 forearc- The Tonga Ridge - 22° to 26° south. In: Stevenson AJ, Herzer RH, Ballance PF

- 637 eds. *Geology and Submarine Resources of the Tonga-Lau-Fiji Region*. SOPAC
638 Technical Bulletin 8. Suva, Fiji, South Pacific Applied Geoscience Commission. Pp.
639 81–99.
640
- 641 Taylor B, Zellmer K, Martinez F, Goodliffe A 1996. Sea-floor spreading in the Lau
642 back-arc basin. *Earth and Planetary Science Letters* 144: 35–40.
643
- 644 Trofimovs J, Amy L, Boudon G et al. 2006. Submarine pyroclastic deposits formed at
645 the Soufriere Hills Volcano, Montserrat (1995–2003): what happens when pyroclastic
646 flows enter the ocean? *Geology*, 34: 549–552.
647
- 648 Trofimovs J, Sparks, RSJ, Talling, PJ 2008. Anatomy of a submarine pyroclastic flow
649 and associated turbidity current: July 2003 dome collapse, Soufriere Hills volcano,
650 Montserrat, West Indies. *Sedimentology* 55: 617–634
651
- 652 Twiss RJ, Moores EM 2007. *Structural Geology*. New York, Freeman. 736 p.
653
- 654 Ui, T 1973. Exceptionally far-reaching, thin pyroclastic flow in Southern Kyushu,
655 Japan. *Bulletin of the Volcanological Society of Japan*. 2 (18): 153–168.
656
- 657 Van Eaton AR, Herzog M, Wilson CNJ, McGregor J 2012. Ascent dynamics of large
658 phreatomagmatic eruption clouds: The role of microphysics. *Journal of Geophysical*
659 *Research - Solid Earth* 117(B3). doi:10.1029/2011JB008892.
660
- 661 Van Eaton AR, Wilson CNJ 2013. The nature, origins and distribution of ash
662 aggregates in a large-scale wet eruption deposit: Oruanui, New Zealand. *Journal of*
663 *Volcanology and Geothermal Research* 250: 129–154.
664
- 665 Walker GPL, Wilson L, Howell ELG 1971. Explosive Volcanic Eruptions I: The Rate
666 of Fall of Pyroclasts. *Geophysical Journal of the Royal Astronomical Society* 22: 377-
667 383
668
- 669 Walker GPL (1981) Plinian eruptions and their products. *Bulletin of Volcanology* 144:
670 223-240.
671
- 672 White JDL, Smellie JL, Clague DA 2003. Introduction: A deductive outline and
673 overview of subaqueous explosive volcanism. *Geophysical Monograph Series, Volume*
674 *140 - Explosive Subaqueous Volcanism*. Pp.1–14.
675
- 676 Wiesner MG, Wang Y, Zheng L 1995. Fallout of volcanic ash to the deep South China
677 Sea induced by the 1991 eruption of Mount Pinatubo. *Geology* 23: 885–888.
678
- 679 Woodhall D 1985. *Geology of the Lau Ridge*. In: Scholl DW, Vallier TL eds. *Geology*
680 *and Offshore Resources of Pacific Island Arcs–Tonga Region*. Earth Science Series 2.
681 Houston, Texas, Circum-Pacific Council for Energy and Mineral Resources. Pp. 351–
682 378.
683
- 684 Wright IC, Gamble JA 1999. Southern Kermadec submarine caldera arc volcanoes (SW
685 Pacific): caldera formation by effusion and pyroclastic eruption. *Marine Geology* 161:
686 207–227.
687
688

689

List of Tables

690

691 **Table 1** Values for U_t , vertical terminal velocity at height, for particles of diameter
692 16 mm and density of 1500 kg m^{-3} , after Pfeiffer et al. (2005).

693

694

695 **Table 2** Dispersal of larger tephra by pyroclastic density currents travelling over the
696 ocean surface (Carey et al. 1996, Allen & Cas 2001, Maeno & Taniguchi 2007, Ui
697 1973). DRE = dense rock equivalent.

698

Cr Peer Review Only

699
700
701
702
703
704
705
706
707
708
709
710
711
712
713
714
715
716
717
718
719
720
721
722
723
724
725
726
727

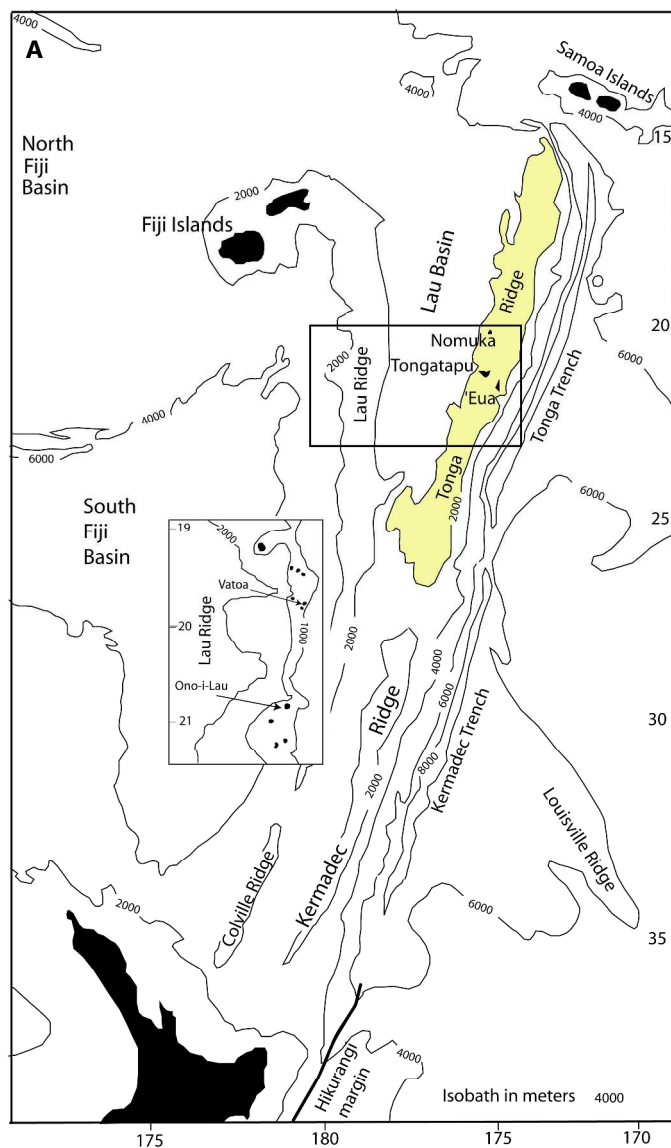
List of Figures

Figure 1 Regional setting. **A**, The position of 'Eua and Nomuka on the Tonga Ridge, and Vatoa and Ono-i-Lau on the Lau Ridge. The Tonga frontal arc basin sediments (shaded) are broadly coincident with the 2000 meter isobath, after Tappin (1993). **B**, The Tonga Ridge platform, highlighted by the 1000 meter isobath, with the currently active back-arc Tofua volcanic chain, with block margins after Tappin et al. (1994), Scholl & Vallier (1985), Austin et al. (1989).

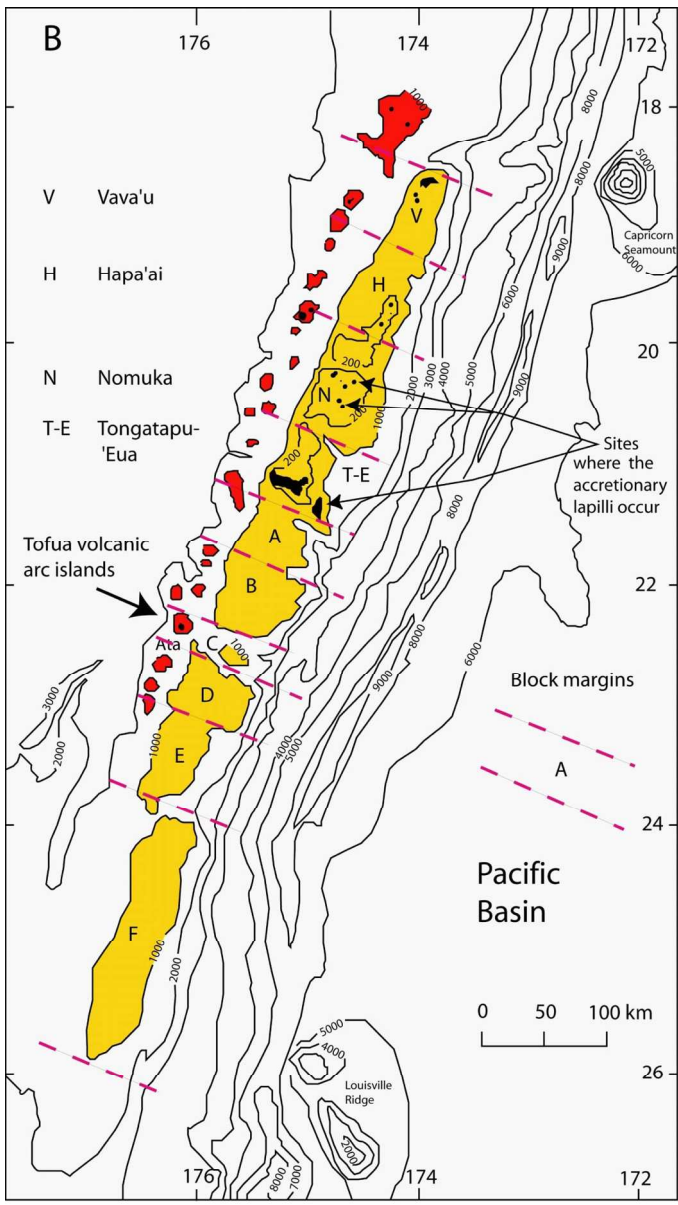
Figure 2 Accretionary lapilli from 'Eua. **A**, Layered accretionary lapilli with coarse ash infill. **B**, Layered accretionary lapilli, some cored, with coarse ash infill. **C**, Rimmed accretionary lapillus. **D**, Rare cross-bed in host volcanoclastics.

Figure 3 Lau Basin tectonics. **A**, Synthesis of data centred on the Lau Basin, after Taylor et al. (1996), with c. 20° easterly rotation of the Tonga Ridge (solid black lines) after Sager et al. (1994). **B**, Outline reconstruction of the ancestral Lau/Tonga ridge, pre-Lau Basin formation, just after splitting commenced, with bathymetric contours. **C**, Schematic section of the Lau Ridge, Lau Basin and Tonga Ridge with ODP sites, at c. 1.5-1.0 Ma, after Clift et al. (1995), modified to reflect the work of Parson & Wright (1996).

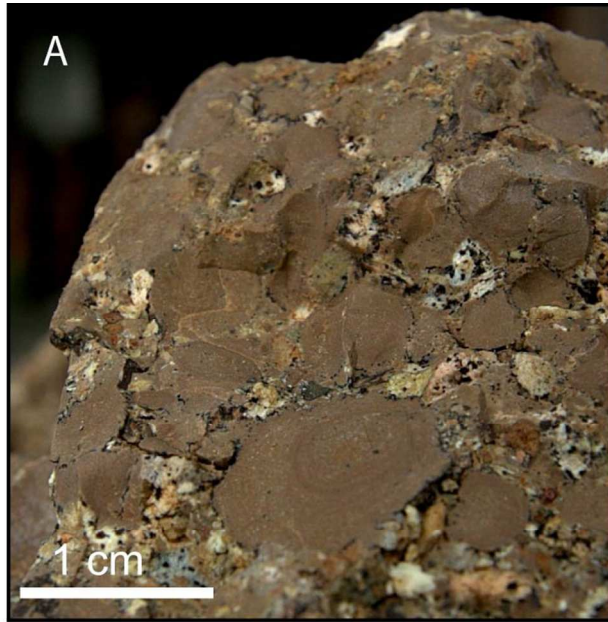
Figure 4. Discontinuity of trends across the boundary between tectonic Blocks A, B and T-E. Trend of gravity and arc basement highs on Blocks A and B is superimposed on residual magnetic anomaly data from Stevenson & Childs (1985), determined by subtracting the 1975 International Geomagnetic Reference Field (IGRF, 1976) from the observed total field measurements. Trend of basement highs on Block T-E is superimposed on total magnetic intensity data from Gatliff et al. (1994).



321x413mm (300 x 300 DPI)

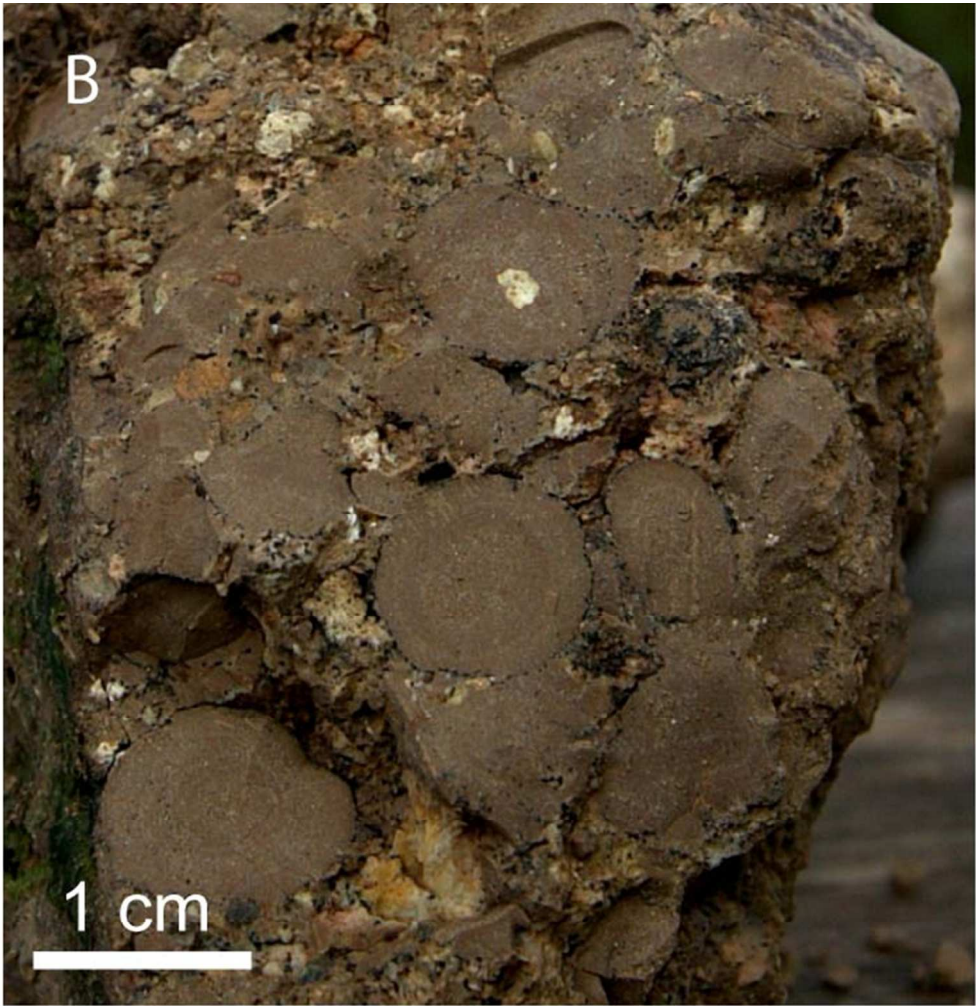


104x172mm (300 x 300 DPI)



98x61mm (300 x 300 DPI)

Review Only



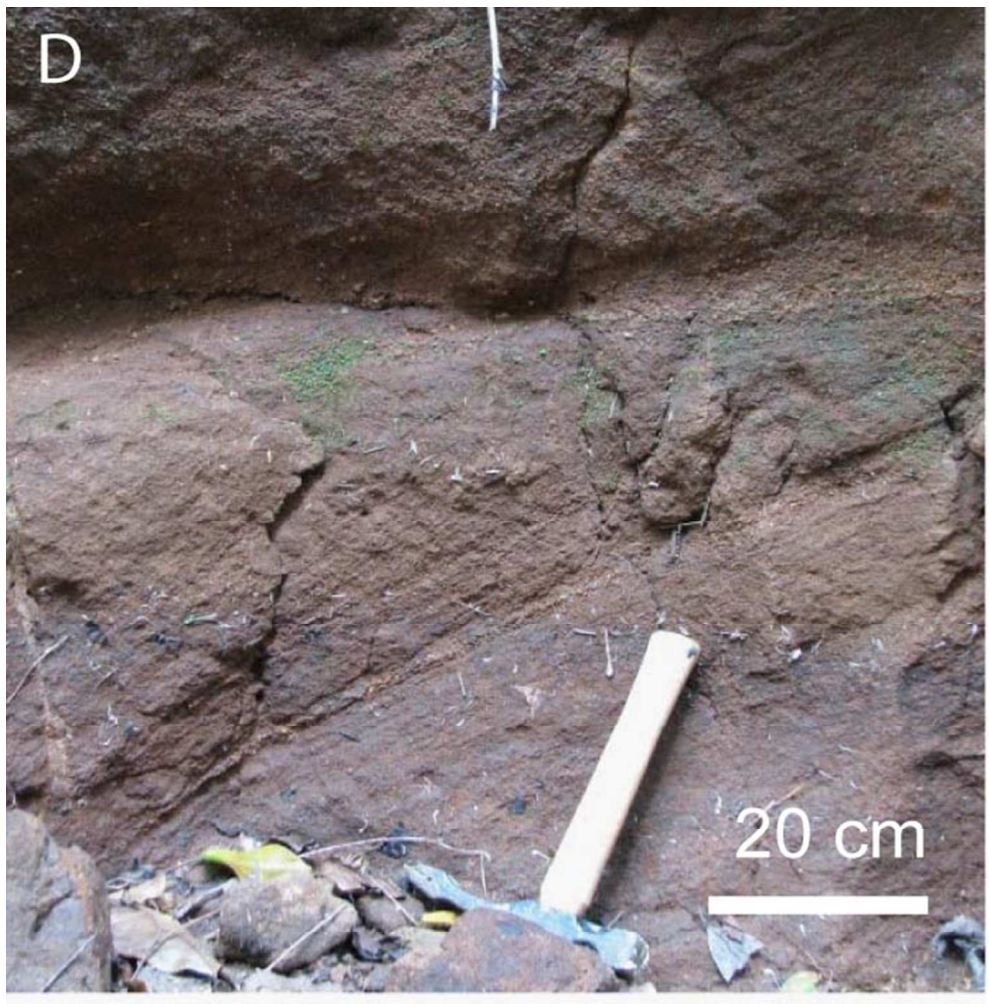
60x61mm (300 x 300 DPI)

Manuscript



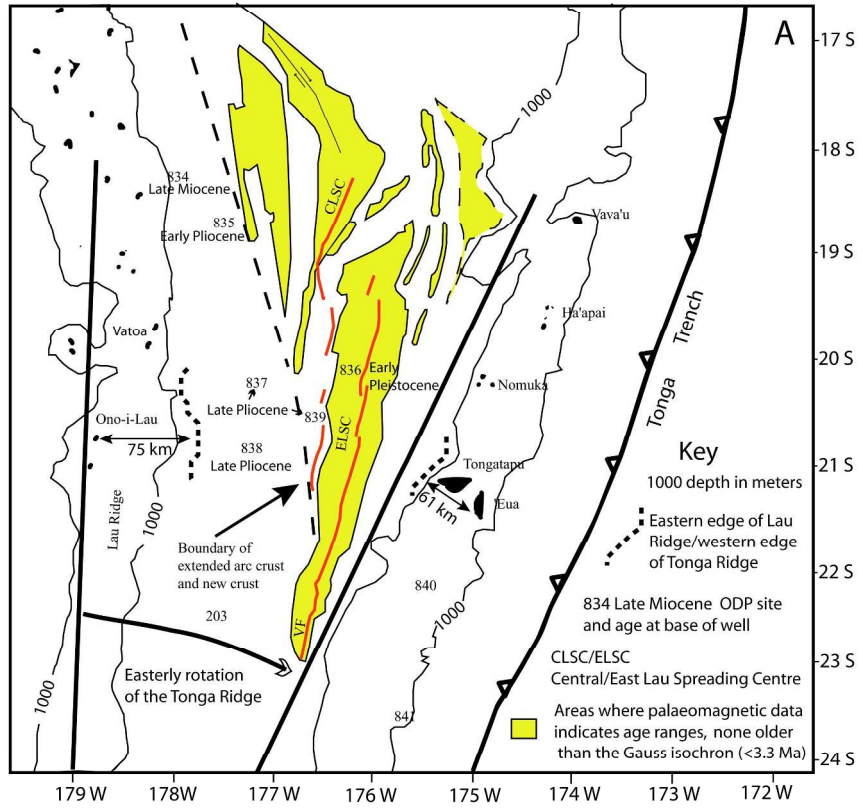
61x59mm (300 x 300 DPI)

Only



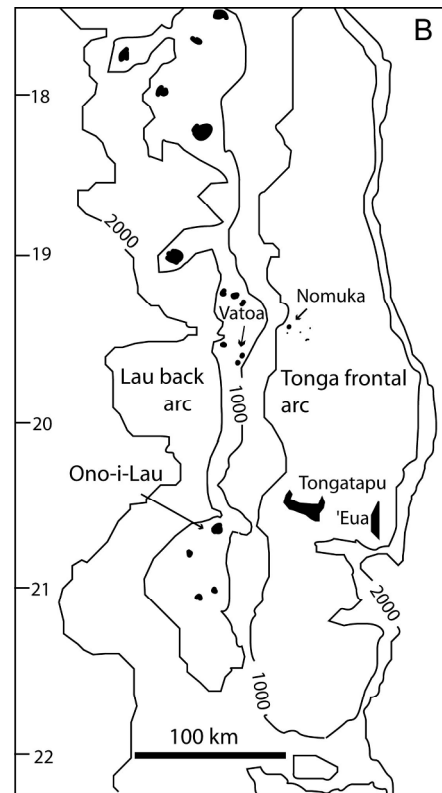
59x61mm (300 x 300 DPI)

Manuscript Central



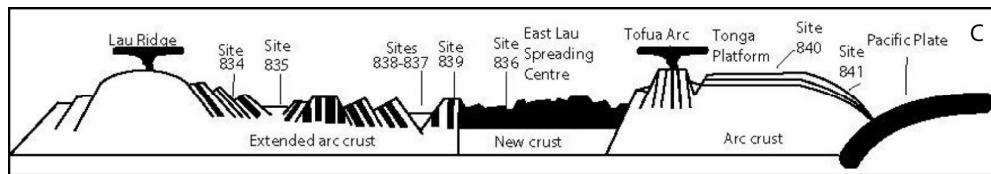
241x229mm (300 x 300 DPI)

Only



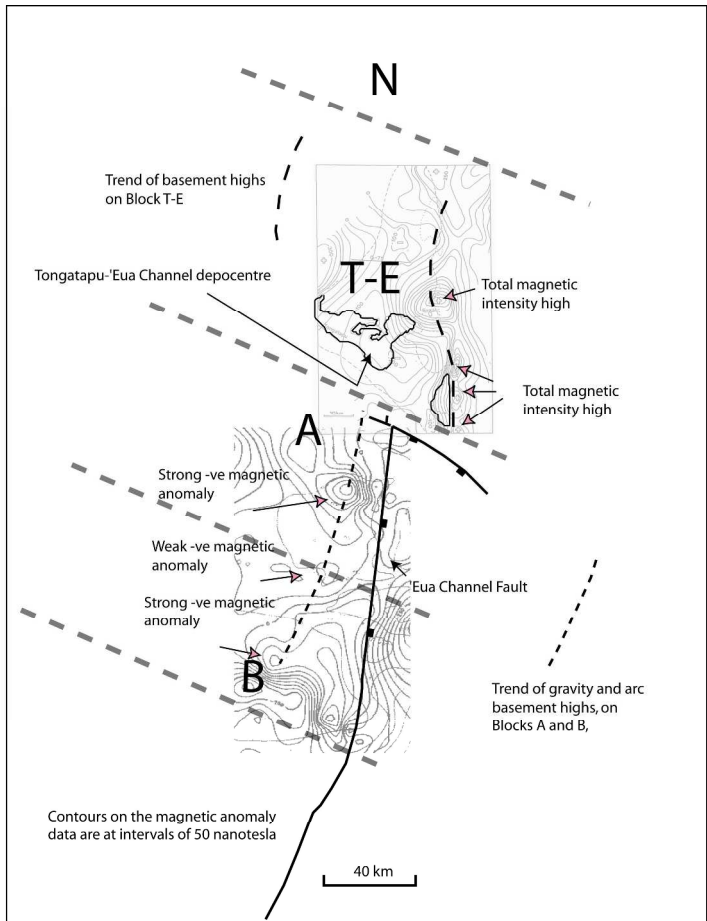
217x171mm (300 x 300 DPI)

new Only



147x25mm (300 x 300 DPI)

For Peer Review Only



273x250mm (300 x 300 DPI)

Only

Height (km)	Sea level	5	15	26
U_t (m sec ⁻¹)	16	20	50	100

For Peer Review Only

Event	DRE (kg m ⁻³)	Larger tephra	Distance from source (km)
Krakatoa	12	pumice stones several centimeters in diameter	65
Kos Plateau Tuff Unit E	30	vent and conduit derived lithic clasts not >200 mm	>60
Kikai Unit D	50	accretionary/armoured lapilli typically 5-9 mm, up to 10 mm	60

For Peer Review Only

~~Sourcing of Middle Miocene accretionary lapilli on 'Eua, Tonga; atypical dispersal distances and their implications.~~

~~Sourcing of Miocene accretionary lapilli on 'Eua, Tonga; atypical dispersal distances and tectonic implications for the central Tonga Ridge.~~

JK Cunningham¹ and AD Beard

Department of Earth and Planetary Sciences, Birkbeck College, University of London, Malet Street London WC1E 7HX

¹ Corresponding author, jcunni1248@aol.com, present address: 1 Loudens Close, St Andrews, Fife, Scotland, KY16 9EN, (44) 1344 479348

Abstract

Volcaniclastics hosting accretionary lapilli on the Tonga Ridge were sourced from the remnant Lau Ridge, prior to Lau back-arc basin opening. For the 'Eua occurrences, an atypical dispersal distance of not less than 70 km is estimated, partly arising from the anomalous easterly position of 'Eua. Dispersal within ocean-surface pyroclastic density currents is supported but strike-slip movement in a fault zone south of 'Eua, post Middle Miocene but pre ridge-splitting, can account for part of the dispersal distance by vertical axis block rotation, a tectonic process common on the southern Tonga-Kermadec-Hikurangi trend. In this model, the volcano which sourced the 'Eua tephra was on a subjacent block, rather than the block which hosts 'Eua. After deposition but prior to the opening of the Lau Basin, the accretionary lapilli on 'Eua became displaced by block rotation c. 40 km towards the Tonga trench and away from source.

Keywords

Accretionary lapilli; Tonga Ridge; dispersal distance; block rotation; pyroclastic density currents.

Introduction

Accretionary lapilli are highly ordered types of ash aggregate typically associated with explosive eruptions, where they may form in the plume itself or in pyroclastic density currents as they interact with the co-ignimbrite ash plume. Dispersal may therefore occur subaerially by expansion of the plume, spreading of any atmospheric umbrella cloud, and/or by pyroclastic density currents. The 'Eua accretionary lapilli contain examples typically 10–15 mm in diameter and are accretionary lapilli *sensu stricto* (Brown et al. 2010, Van Eaton & Wilson 2013), as distinguished from less ordered ash pellets and fragile ash aggregates (Brazier et al. 1982; Carey & Sigurdsson 1982; Wiesner et al. 1995; Brown et al. 2012) which rarely survive in that form but are detected in sieve analysis of grain size.

Formatted: Line spacing: single, Tab stops: Not at 2.25"

50 Accretionary lapilli have been reported from Miocene volcanoclastics which are exposed
51 on the Nomuka group islands (Ballance et al. 2004) and on 'Eua on the Tonga Ridge
52 (Ballance et al. 2004; Cunningham & Beard 2014). The host volcanoclastics were
53 sourced from volcanoes on the Lau Ridge, prior to the splitting of the Lau-Tonga
54 ancestral arc in the latest Late Miocene to form the Lau back-arc basin (Clift et al.
55 1994, 1995, 1998; Cole et al. 1985; Parson & Wright 1996). Reconstruction of the
56 ancestral ridge places the Nomuka group islands, which are positioned on the west of
57 the Tonga Ridge, at modest dispersal distances from potential source. However, 'Eua is
58 the most easterly of the island exposures along the Tonga Ridge by some margin and
59 this contributes to a dispersal distance from source at the limit of most (but not all)
60 documented occurrences of accretionary lapilli. The resolution of the two problems
61 presented by the anomalous position of 'Eua and the exceptional distance from potential
62 source of the accretionary lapilli found on 'Eua is the focus of this paper.

63 ~~While the Tonga Ridge has acted as one microplate during the Lau Basin opening~~
64 ~~process (Sager et al. 1994), it comprises a number of fault bounded blocks. These~~
65 ~~blocks have moved differently *inter se* during tectonic events, revealed by~~
66 ~~seismostratigraphy (Scholl & Vallier 1985; Stevenson et al. 1994). Rotation of the block~~
67 ~~hosting 'Eua provides a potential tectonic explanation for the anomalous position of 'Eua~~
68 ~~and the unusual dispersal distance of the 'Eua accretionary lapilli from source. However~~
69 ~~the Tonga-Kermadec-Hikurangi trend further south provides evidence for both block~~
70 ~~rotation and unusual dispersal distances for accretionary lapilli (Lamb 2011, Van Eaton~~
71 ~~& Wilson 2013).~~

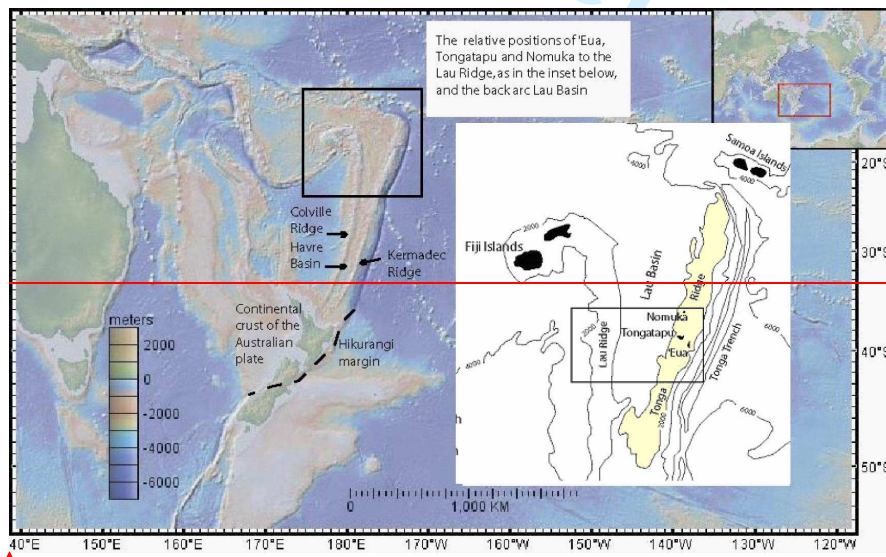
72 The approach taken ~~in this paper~~ to address the two problems is ~~firstly firstly~~ to use data
73 from the Tonga Ridge, the Lau Basin and the Lau Ridge to constrain possible locations
74 for the Middle Miocene source volcano which provided the accretionary lapilli on 'Eua,
75 to consider how the distance between source and destination may have been impacted
76 by post Middle Miocene tectonics, including block rotation, and to estimate the
77 minimum actual contemporary distance from source. Thereafter, the paper examines
78 constraints on possible maximum dispersal distances for the relatively large
79 accretionary lapilli from 'Eua. ~~The evidence for block rotation on the central Tonga~~
80 ~~Ridge is then presented, and the actual relative displacement of 'Eua arising from~~
81 ~~tectonism alone deduced.~~ Discussion is then enabled on whether the anomalous
82 position of 'Eua and the unusual dispersal distance of the 'Eua accretionary lapilli from
83 source can be explained by block rotation within the Tonga microplate and/or a

84 dispersal distance enabled by a pyroclastic density current which traversed the ocean
 85 surface before depositing the accretionary lapilli on 'Eua, ~~or whether a Middle Miocene~~
 86 ~~ultra-Plinian explosive volcanic event on the ancestral Lau-Tonga Ridge must be~~
 87 ~~invoked.~~

88 Regional setting

89 ~~Located on the northern part of the Hikurangi-Kermadec-Tonga trend, the Tonga and~~
 90 ~~Lau Ridges are dominantly open marine, as delineated by the 2000 meter contour (Fig.~~
 91 ~~1A). A number of islands occur, some large, but most are barely emergent and~~
 92 ~~exposures are limited. On the Tonga Ridge, the island of 'Eua is an exception, where an~~
 93 ~~uplifted Eocene basement high and overlying sediments are now exposed subaerially.~~
 94 ~~These sediments include deep marine Middle Miocene volcanoclastics. The study area~~
 95 ~~of the SW Pacific (Fig. 1) is a tectonic province with a relatively well-documented~~
 96 ~~geological history, particularly with respect to back-arc extension/basin formation~~
 97 ~~processes (Paekham 1978; Tappin 1993; Sager et al. 1994; Tappin et al. 1994; Parson~~
 98 ~~and Wright 1996; Taylor et al. 1996). In the south of the region, on the Tonga-~~
 99 ~~Kermadec-Hikurangi trend, subducting oceanic plate encounters continental crust on~~
 100 ~~South Island, New Zealand (Lamb 2011). Further north, the environment is oceanic.~~

101



102

103

104 **Figure 1.** — The position of the Lau Basin on the north end of the Tonga-Kermadec-
 105 Hikurangi trend and the study area. The Tonga frontal-arc basin sediments (shaded) are
 106 broadly coincident with the 2000 meter isobath, after Tappin (1993). Base map from
 107 GeoMapApp, <http://www.geomapp.org>.

Formatted: Font color: Black

Formatted: Font color: Black

Formatted: Font color: Black

Formatted: Font color: Black

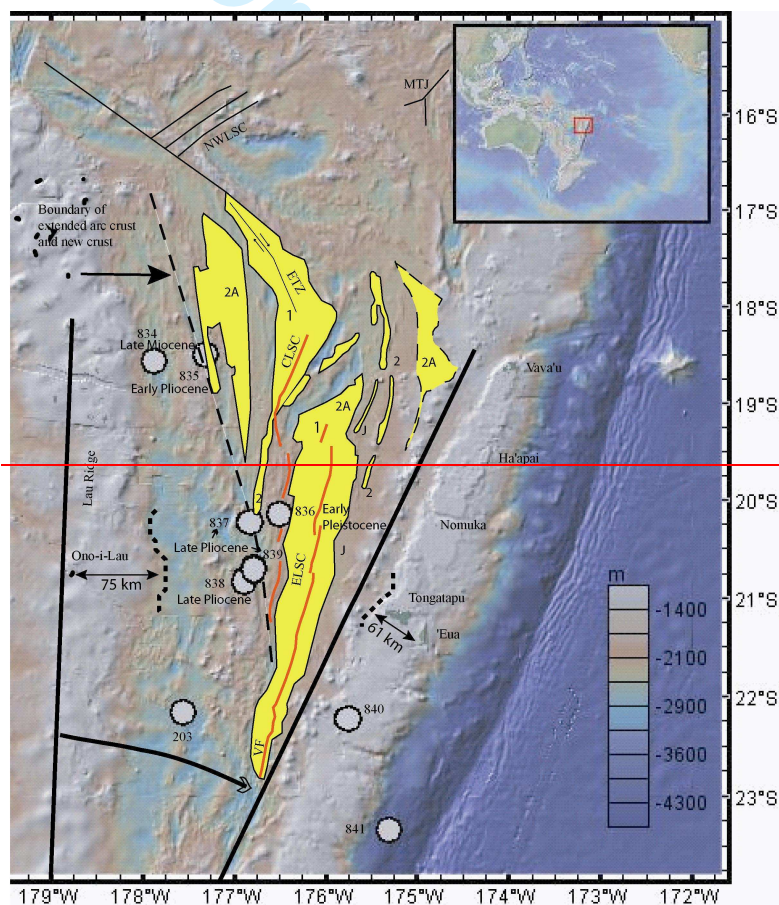
Formatted: Font color: Black

Formatted: Font color: Black

Formatted: Font color: Black

108
109
110
111
112
113
114
115

A more sophisticated model for Lau Basin formation (Fig. 2-3) replaced a simple mid-oceanic type spreading centre model with a two-phase model (Parson et al. 1994; Parson & Wright 1996; Taylor et al. 1996). The Lau basin floor geology is asymmetric; patterns of strong positive magnetic intensity are exhibited east of a line running NNE across the Lau Basin at roughly 317 degrees, reflecting the new oceanic crust being created at the Central and Eastern Lau spreading centres



116
117
118
119
120
121
122
123
124

Figure 2. Synthesis of data centred on the Lau Basin, after Taylor et al. (1996), with c. 20° easterly rotation of the Tonga Ridge (solid black lines) after Sager et al. (1994), base map from GeoMapApp, <http://www.geomapapp.org>. Extended legend as follows:

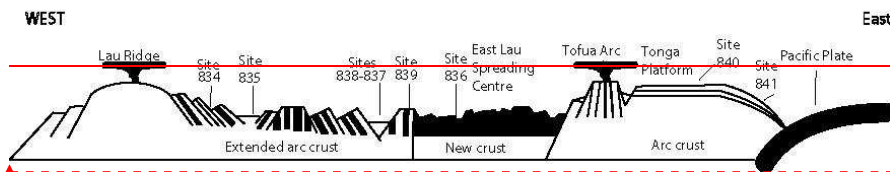
- 834 Late Miocene — ODP site and age at base of well
- Lighter areas (2A) — Areas where palaeomagnetic data correlates with known age ranges, none older than the Gauss isochron (<3.3 Ma)

Formatted: Font color: Black
Formatted: Tab stops: 1", Left + 1.13", Left + 1.5", Left
Formatted: Font color: Black

Formatted: Font color: Black
Formatted: Font color: Black

- 125 1, 2, 2A ————— Subdivisions of isochrons
 126 J ————— Jaramillo isochron
 127 CLSC/ELSC ————— Central Lau Spreading Centre/East Lau Spreading Centre
 128 ETZ/NWSLC/MTJ ————— Extensional Transform Zone/ NW Lau Spreading
 129 Centre/Mangatolo Triple Junction
 130 Dashed line ————— West of this line, is the “extended ancestral arc crust”
 131 —————
 132 Dotted line ————— Eastern edge of Lau Ridge/western edge of Tonga Ridge
 133

134 However west of that line and east of the 2000 meter isobath on the Lau Ridge, an
 135 irregular terrain of north trending horst/grabens occurs where specific magnetization
 136 events were not well delineated, attributed to diffuse spreading to form “extended arc
 137 crust” (Fig. 3):



138
 139 **Figure 3.** — Schematic section of the Lau Ridge, Lau Basin and Tonga Ridge with
 140 ODP sites, at c. 1.5–1.0 Ma, after Clift et al. (1995), modified to reflect the work of
 141 Parson and Wright (1996):

142
 143 In broad terms, the ancestral Lau/Tonga Ridge arc crust split and experienced extension
 144 to the east of the active arc volcanoes on the remnant Lau Ridge by:

- 145 • graben/half graben faulting accompanied by intrusive activity which mark the
 146 location of repeated “failed” spreading centres (creating the “extended arc
 147 crust”), before:
- 148 • formation of new crust occurred continuously at more typical mid-ocean ridge
 149 type spreading centres (the Central Lau Spreading Centre/East Lau Spreading
 150 Centre (Fig. 2), which were initiated in the north of the Lau Basin and
 151 propagated southwards.

152 During these processes, Lau Ridge and intra-basin volcanism occurred and eventually
 153 ceased, before restoration of back arc volcanism on the currently active Tofua Arc (Fig.
 154 3–4). The net effect is that of an apparent rotation of the Tonga Ridge, the current active
 155 arc, some 20° clockwise, away from the remnant Lau Ridge segment of the ancestral
 156 arc.

157 **The Tonga Ridge and the remnant Lau Ridge**

158

Formatted: Font color: Black

Formatted: Font color: Black

Formatted: Line spacing: single, Pattern: Clear

Formatted: Bullets and Numbering

159 More is known of the Tonga Ridge (Fig. 1B) than the remnant Lau Ridge. Oil industry
 160 activity, including 5 exploration wells on Tongatapu, proved that a deep basin of
 161 sediment overlies a presumed volcanic arc basement on the north-central part of the
 162 Tonga Platform (Cunningham and Anscombe 1985). Scientific cruises (Scholl and
 163 Vallier 1985, Stevenson et al. 1994) confirmed this frontal arc basin extended south and
 164 established that the present Tonga Ridge is broken into a number of fault-delineated
 165 blocks (Fig. 1B4).

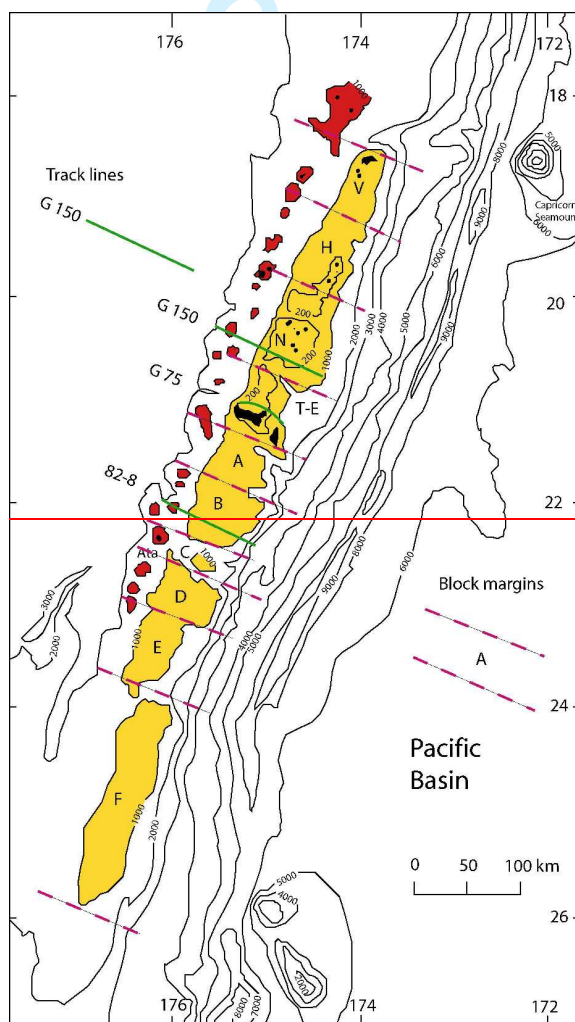
Formatted: Font color: Black

Formatted: Font color: Black

Formatted: Font color: Black

Formatted: Font color: Black

Formatted: Font color: Black



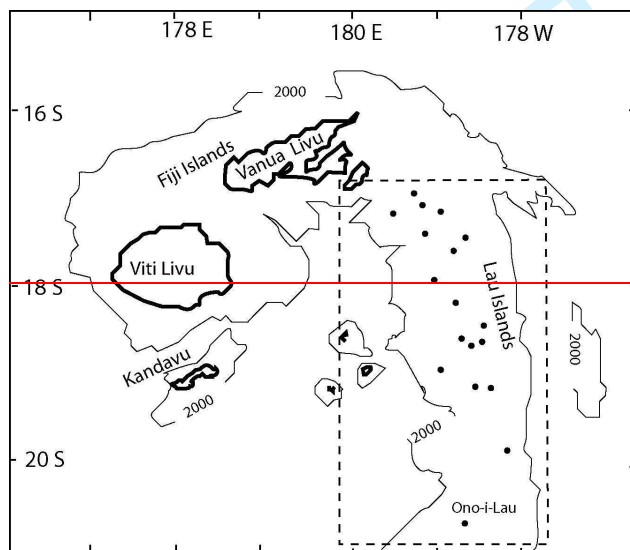
166

167

168 **Figure 4.** — The Tonga Ridge platform, highlighted by the 1000 meter isobath, with
 169 the currently active back arc Tofua volcanic chain, with block margins and selected
 170 track lines, after Tappin et al. (1994), Scholl and Vallier (1985), Austin et al. (1989),
 171 Lehner et al. (1983).

172
 173 ~~Supplementary Information A published online provides a more detailed overview of~~
 174 ~~the seismostratigraphic features and interpreted history of the Tonga Ridge frontal are~~
 175 ~~basin.~~ On the southern platform, depocentres are identifiable on the west of the basin
 176 on isopach A–B (which includes the Miocene), with the sediments thickening generally
 177 towards the west. Herzer & Exon (1985) suspected that their alignment along the west
 178 side of the basin indicated these sediment "thicks" were fed from volcanic centeres
 179 "nearby to the west, outside the mapped area".

180
 181 The Lau Ridge bathymetry is very similar to the Tonga Ridge, broadly outlined by the
 182 2000 meter contour (Fig. ~~-1A5 and Supplementary Information B~~), but many more
 183 islands with a dominantly volcanic aspect dominate the geology (Woodhall 1985).
 184 Basement rocks are not exposed in the islands, the oldest rocks exposed being Middle
 185 Miocene, but volcanism extended from 14.0 to <2.5 Ma, so older geology would have
 186 been obscured on volcanic islands.
 187
 188



189
 190
 191 **Figure 5.** — Fiji and the Lau islands, after Cole et al. (1985), bathymetric contour
 192 interval 2000 meters. The inset box outlines the Lau Islands whose geology was
 193 reported by Woodhall (1985), the most southerly of which is Ono-i-Lau.
 194

195 Thus the many Lau Islands which have a long-lived volcanic history provide credible
 196 candidates for the volcanic centeres "nearby to the west, outside the mapped area" of
 197 Herzer & Exon (1985). The island arc andesite character of the Lau Volcanic group

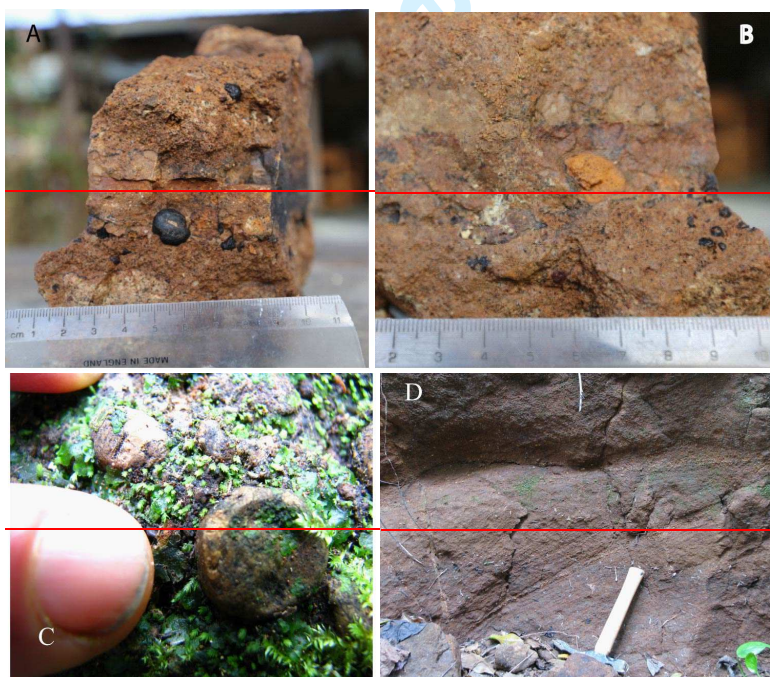
198 (14.0–6.0 Ma) and the age range which includes the Middle Miocene, the age of the
 199 mafic volcanoclastics on 'Eua, supports the case. In order to provide a working model
 200 for the sourcing of the accretionary lapilli found on the Tonga Ridge, it is now
 201 necessary to constrain possible source locations prior to the Tonga Ridge segment
 202 partition of the ancestral Lau-Tonga Ridge and then consider how the active tectonics in
 203 the region may have re-positioned source or settlement site, hosting a deep sedimentary
 204 basin of dominantly volcanoclastic sediment, fed from volcanoes on the remnant Lau
 205 Ridge pre-splitting, provides a working model for sourcing of the accretionary lapilli
 206 found on the Tonga Ridge.

207

208

209 The accretionary lapilli and the location of possible volcanic sources

210



211

212

213

214

215

216

217

218 The rThe reported occurrences of accretionary lapilli on the Tonga Ridge are from

219 Miocene ~~marine~~ volcanoclastics on 'Eua and on from two islands in the Nomuka group

Formatted: Line spacing: 1.5 lines

Formatted: Line spacing: 1.5 lines

Formatted: Line spacing: single, Pattern: Clear

220 (Fig. 1B). The 'Eua occurrences (Fig. 2A–C) range up to 20 mm in maximum
221 dimension and typically occur unsorted in grain to grain contact as thin beds up to 20
222 cm in thickness. The matrix is coarse-grained (>500 µm) or absent. The 'Eua
223 occurrences exhibit characteristics suggesting they settled to pelagic depths (Ballance et
224 al. 2004; Cunningham & Beard 2014) while some of the Nomuka occurrences may have
225 been reworked from the original settlement site (Ballance et al. 2004). The 'Eua host
226 volcanoclastics are typically granulestone/sandstone in grain size, with occasional larger
227 clast sizes, none in excess of 320 mm, and a pelagic planktonic foraminiferal fauna. The
228 fauna are dated at Middle Miocene, c. 14 Ma, with sparse re-worked slightly earlier
229 fauna (Quinterno 1985; Chaproniere 1994), indicating depths of deposition are not less
230 than 1600 meters. A range of sediment gravity flow types (Ballance et al. 2004) are
231 reflected in the host formation, with rare westwards-dipping ~~had~~ cross-beds (Fig.
232 26D). Tappin & Ballance (1994) reported a WNW ~~verging~~ flame structure. In
233 contrast, the 'Eua beds of accretionary lapilli exhibit a narrow size distribution in that
234 they are large, typically 10-15 mm in diameter, and the matrix is fines-depleted or
235 absent. These features are applied to terminal velocity calculations by Cunningham &
236 Beard (2014) to argue that these beds were the result of settling to pelagic depths and
237 were not delivered by sediment gravity flows or submarine pyroclastic flows. The upper
238 size constraint of volcanogenic clasts in the 'Eua volcanoclastics contrasts with the
239 Nomuka host rocks: on Mango in the Nomuka group of islands. Middle (?) Miocene
240 volcanoclastics contain indications of the proximity of volcanic edifices, such as
241 volcanic boulder-bearing debris flow deposits (Ballance et al. 2004). ~~Detecting the~~
242 Further south on the T–E block, the detection of volcanic sources is assisted by the
243 availability of close-spaced oil industry data (Gatliff et al. 1994). With the high rates of
244 sediment supply implicit in island arc environments, the problem of distinguishing reef
245 structures from buried volcanic edifices is important and has been reviewed (Alexander
246 1985; Herzer & Exon 1985; Pflueger & Havard 1994; Tappin et al. 1994). Only one
247 volcanic edifice was detected along the Tonga Ridge, in the B–C Late Oligocene to
248 Early Miocene interval and on Block D. No ambiguous structures at all were identified
249 on the T–E block within the interval which includes the Middle Miocene (Gatliff et al.
250 1994) and “No volcanic structures sourcing unit A–B have yet been identified on the
251 Tonga Ridge” (Tappin et al. 1994). ~~In contrast, some of the host volcanoclastics in the~~
252 Nomuka group contain evidence of shallow water/proximal volcanic activity, including
253 boulder-sized volcanic clasts. ~~However~~ ~~†~~ Thus the seismostratigraphy reveals no obvious

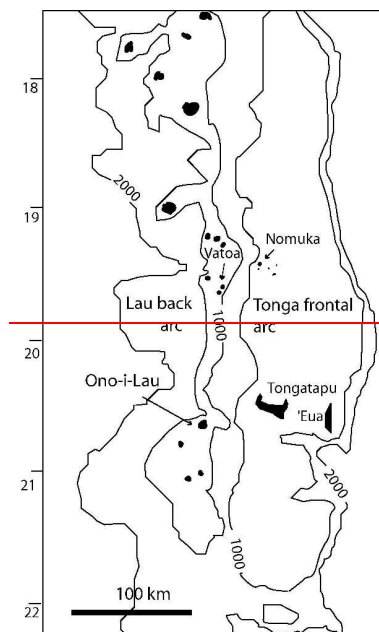
Formatted: Font color: Black

254 local source on the Tonga Ridge for the accretionary lapilli, either for the Nomuka
255 group or the 'Eua occurrences.

256 The regional setting suggests that sources would be to the west and on the remnant Lau
257 Ridge, where long-lived volcanic islands exist. ~~The present 1000 meter contour on the
258 Lau Ridge marks commencement of descent to the Lau Basin floor. On the Tonga
259 Ridge, the present 1000 meter contour on the western flank marks commencement of
260 the steep descent to the Tofua Basin floor and steep faults having westwards appear on
261 most of the seismic lines which cross this contour.~~

262 ~~Using these present sea bed depth contours at 1000 and 2000 meters to estimate the
263 width of the ancestral arc elements, an outline reconstruction (Fig. 7) is achieved by
264 rotating the Tonga Ridge in the horizontal plane back to the west by the c. 20°
265 estimated by Sager et al. (1994).~~

266
267



268
269

270 **Figure 7.** — Outline reconstruction of the ancestral Lau/Tonga ridge, pre-Lau Basin
271 formation, just after splitting commenced.

272

273 In the reconstruction, Ono-i-Lau is closest to 'Eua and Vatoa close to most of the
274 Nomuka group islands. If the gap between the subjacent 1000-meter contours is closed,

275 a potential Lau Ridge source for the 'Eua Middle Miocene volcaniastics, located in the
276 region of Ono i Lau, would be at a distance of perhaps a little over 90 km from 'Eua.
277 Even with the high margin of error implicit in the reconstruction, 'Eua appears to be at a
278 considerable distance from a Lau island source. This ignores crustal extension of the
279 ancestral arc elements since the Lau Basin opening, but the Tonga Ridge
280 seismostratigraphy suggests little post-Miocene fault movement on ridge-parallel faults.
281 In contrast, the Nomuka group islands, being on the western edge of the Tonga Ridge,
282 are much closer to the Lau Ridge islands. On Mango in the Nomuka group of islands,
283 Middle (?) Miocene volcaniastics contain indications of the proximity of volcanic
284 edifices, such as volcanic boulder-bearing debris flow deposits (Ballance et al. 2004).
285 The possibility of the 'Eua source being much nearer, in the western Lau Basin extended
286 arc crust (Fig. 2) or even on the Tonga Ridge itself must be considered. However,
287 evidence of a proximal source in the ancestral Lau-Tonga Ridge segments of the
288 extended arc crust of the western Lau Basin is not available; the ODP sites in the
289 western Lau Basin encountered dates no earlier than Late Miocene at Site 834 and
290 hence possible volcanic edifices, even if identifiable, cannot be dated. In contrast, the
291 data along the Tonga Ridge is rich, and in particular on the T-E block where close-
292 spaced oil industry data is available (Gatliff et al. 1994). With the high rates of sediment
293 supply implicit in island arc environments, the problem of distinguishing reef structures
294 from buried volcanic edifices is important and has been reviewed (Alexander 1985;
295 Herzer & Exon 1985; Pflueger & Havard 1994; Tappin et al. 1994). Only one volcanic
296 edifice was detected along the Tonga Ridge, in the B-C Late Oligocene to Early
297 Miocene interval and on Block D. No ambiguous structures at all were identified on the
298 T-E block within the interval which includes the Middle Miocene (Gatliff et al. 1994).
299 The seismostratigraphy provides sparse vestigial evidence for a Miocene source actually
300 on the Tonga Ridge segment of the ancestral arc; the east-dipping clinoform reflectors
301 within the A-B Middle to Late Miocene interval further south on Block D (see
302 Supplementary Information A) could be interpreted as a volcanic flank structure. But
303 earlier workers would disagree; "No volcanic structures sourcing unit A-B have yet
304 been identified on the Tonga Ridge" (Tappin et al. 1994).

305

306 **Constraining distance from source for the 'Eua occurrences:**

307 With no compelling evidence to support a source on the Tonga Ridge, 'Eua appears to
308 be at a considerable distance from a source which must have existed further to the west

309 on the ancestral Lau-Tonga ridge. The geological record often preserves only vestigial
310 remnants of any source volcanic edifice. The difficulties of locating the source of
311 tephra for non-historic volcanic events are increased by the high impact of tectonism in
312 this area of the Pacific. However, by using the seismostratigraphic record, we can at
313 least constrain the minimum distance from source of the 'Eua tephra by summing the
314 ancestral arc segments.

315 **The Tonga segment**

316 On Block T-E, the distance between the western edge of the Tonga Ridge and 'Eua,
317 where it thins against the proto-'Eua submergent high is c. 61 km (Fig. 2), before
318 correction for extension due to post-Middle Miocene faulting. Post-Middle Miocene
319 sub-vertical fault patterns on the Tonga Ridge segment do not suggest this will be
320 material, when compared with pre-Middle Miocene graben/half-graben faulting which
321 may be listric at depth. However the threat of underestimation of extension due to
322 unidentified small faults (Twiss & Moores 2007), supports the application of a non-
323 trivial provision, say $\beta = 1.1$, which would bring the 61 km estimate down to c. 55 km
324 pre-fault extension. The Tonga frontal arc basin segment terminates abruptly on the
325 west with down-to-Tofua faulting (Supplementary Information A). The footprint of any
326 volcanic source on the remnant Lau Ridge segment requires estimation. The profile of
327 the currently active Tofua arc volcanoes provide possible analogues of Lau Ridge
328 volcanic sources. At base, these range up to c. 30 km in width, excluding composite
329 structures which are wider (Chase 1985, Fig. 1). On this basis, 55 plus 15 km = 70 km is
330 indicative of the minimum distance from a source on the eastern edge of the remnant
331 Lau Ridge segment.

332 **The remnant Lau segment**

334 If the source volcano was originally in what is now the extended arc crust of the western
335 Lau Basin and not in the position of Ono-i-Lau on the Lau Ridge (Fig. 2), this
336 component could be as low as the 15 km estimate for the source edifice already made
337 above. A much higher figure is required however if a structure in the position of Ono-i-
338 Lau is considered. In the Lau Basin at the longitude under study c. 105 km of extended
339 arc crust exists and the distance from Ono-i-Lau to the eastern edge of the Lau Ridge is
340 75 km (Fig. 2). However a significant number of detectable faults exist on the Lau
341 Ridge (Woodhall 1985) and in the Lau Basin extended arc crust. Adjustment for crustal
342 extension is therefore again required. Faults may be listric at depth and Parson and

343 Wright (1996) consider arguments for a $\beta = 3$. Applying $\beta = 3$ to the total extended arc
344 and Lau Ridge crust, 60 km remains as the minimal distance from source of the remnant
345 Lau segment.

346 Combining the two ancestral components on a Ono i Lau source scenario provides a
347 minimum 60 km for the Lau Ridge and the extended arc "slivers" in the Lau Basin, plus
348 a post Middle Miocene extension adjusted 55 km for the Tonga Ridge segment to give
349 a total of 115 km, which is in range of the estimate of 90 km made on the basis of the
350 outline reconstruction (Fig.7). A minimum of 70 km in total is provided by the scenario
351 where the edifice was close to the eastern edge of the Lau Ridge segment.

352 Tectonics

353 The study area of the SW Pacific is a tectonic province with a relatively well-
354 documented geological history, particularly with respect to back-arc extension/basin
355 formation processes (Packham 1978; Tappin 1993; Sager et al. 1994; Tappin et al.
356 1994; Parson and Wright 1996; Taylor et al. 1996). In the south of the region, on the
357 Tonga-Kermadec-Hikurangi trend, subducting oceanic plate encounters continental
358 crust on South Island, New Zealand (Lamb 2011). Further north, the environment is
359 oceanic. A more sophisticated model for Lau Basin formation (Figs. 3A, 3C) replaced a
360 simple mid-oceanic type spreading centre model with a two-phase model (Parson et al.
361 1994; Parson & Wright 1996; Taylor et al. 1996). The Lau basin floor geology is
362 asymmetric; patterns of strong positive magnetic intensity are exhibited east of a line
363 running NNW across the Lau Basin at roughly 317° , reflecting the new oceanic crust
364 being created at the Central and Eastern Lau spreading centres. However, west of that
365 line and east of the 2000 meter isobath on the Lau Ridge, an irregular terrain of north-
366 trending horst/grabens occurs where specific magnetization events were not well
367 delineated, attributed to diffuse spreading to form "extended arc crust". In broad terms,
368 the ancestral Lau/Tonga Ridge arc crust split and experienced extension to the east of
369 the active arc volcanoes on the remnant Lau Ridge by:

- 370 • graben/half-graben faulting accompanied by intrusive activity which mark the
371 location of repeated "failed" spreading centres (creating the "extended arc
372 crust"), before:
- 373 • formation of new crust occurred continuously at more typical mid-ocean ridge
374 type spreading centres (the Central Lau Spreading Centre/East Lau Spreading
375 Centre, which were initiated in the north of the Lau Basin and propagated
376 southwards.

Formatted: Bullets and Numbering

377 During these processes, Lau Ridge and intra-basin volcanism occurred and eventually
378 ceased, before restoration of back-arc volcanism on the currently active Tofua Arc. The
379 net effect is that of an apparent rotation of the Tonga Ridge, the current active arc, some
380 20⁰ clockwise, away from the remnant Lau Ridge segment of the ancestral arc. With no
381 compelling evidence to support a source on the Tonga Ridge, 'Eua appears to be at a
382 considerable distance from a source which must have existed further to the west on the
383 ancestral Lau-Tonga ridge. Using present sea-bed depth contours at 1000 and 2000
384 meters to estimate the width of the ancestral arc elements, an outline reconstruction
385 (Fig. 3B) is achieved by rotating the Tonga Ridge in the horizontal plane back to the
386 west by the c. 20⁰ estimated by Sager et al. (1994). On Block T-E, the distance
387 between the western edge of the Tonga Ridge and 'Eua, where it thins against the proto-
388 'Eua submergent high is c. 61 km (Fig. 3A), before correction for extension due to
389 post-Middle Miocene faulting. Post-Middle Miocene sub-vertical fault patterns on the
390 Tonga Ridge segment do not suggest this will be material, when compared with pre-
391 Middle Miocene graben/half graben faulting which may be listric at depth. However,
392 the threat of underestimation of extension due to unidentified small faults (Twiss &
393 Moore's 2007), supports the application of a non-trivial provision, say 10%, which
394 would bring the 61 km estimate down to c. 55 km pre-fault extension. The Tonga
395 frontal arc basin segment terminates abruptly on the west with down-to-Tofua faulting
396 (Herzer & Exxon 1985). The footprint of any volcanic source on the remnant Lau Ridge
397 segment requires estimation. The profile of the currently active Tofua arc volcanoes
398 provide possible analogues of Lau Ridge volcanic sources. At base, these range up to c.
399 30 km in width, excluding composite structures which are wider (Chase 1985, Fig. 1).
400 On this basis, 55 plus 15 km = 70 km is indicative of the minimum distance from a
401 source on the eastern edge of the remnant Lau Ridge segment. If the source volcano
402 was originally in what is now the extended arc crust of the western Lau Basin, this
403 figure is increased, but no data is available from the ODP sites in the Lau Basin to
404 constrain this possibility, as none of these reached the Middle Miocene (Fig. 3A). A
405 much higher figure is required if a structure in the position of Ono-i-Lau is considered.
406 In the Lau Basin at the longitude under study, c.105 km of extended arc crust exists and
407 the distance from Ono-i-Lau to the eastern edge of the Lau Ridge is 75 km.
408 The more local effects of individual block rotation are now considered. During re-
409 processing of oil industry data on the T-E Block, it was noted that a number of
410 physiographic features of the block would be explained if it had rotated 30⁰

411 anticlockwise (Gatliff et al. 1994). One feature is the atypical triangular shape of the
412 Tongatapu-‘Eua block as a whole (Fig. 1B), as reflected at the 1000 m isobath. ‘Eua is
413 closer to the eastern margin of the frontal arc basin than any other basement high, and as
414 an emergent island with an elevation of 912 meters, is much higher. To further explore
415 whether there is seismostratigraphic/geophysical support for the rotation proposition, a
416 number of sources of data were superimposed on Blocks A, B and T–E (Fig. 4). There
417 are clearly a number of departures from the Tonga Ridge NNE-SSW ridge-parallel
418 structural trend, localised to the southern margin of Block T–E. On Block T–E, a trend
419 in total magnetic intensity highs, broadly coincident with basement highs (Gatliff et al.
420 1994) departs from trend and is deflected east of ‘Eua. Further south, on Blocks A and
421 B, a trend of magnetic intensity anomalies (Stevenson & Childs 1985), coincident with
422 ridge-parallel gravity/basement highs, is abruptly curtailed as the southern margin of the
423 T–E block is encountered. The ‘Eua Channel Fault, a major structural feature on the
424 southern Tonga Ridge, disappears north of the Block T–E southern margin, where the
425 Tongatapu/‘Eua Channel depocentre was identified (Herzer and Exon 1985, Gatliff et
426 al. 1994).

427 The three total magnetic intensity highs immediately east of ‘Eua on the Tongatapu-
428 ‘Eua block appear to be displaced by a strike-slip fault c. 40 km to the east of the trend
429 of the magnetic intensity anomalies on Blocks A and B. This would have the effect of
430 anticlockwise rotation *sensu* Gatliff et al. (1994). Further south on the Tonga-
431 Kermadec-Hikurangi trend, Lamb (2011) reviews the tectonics and kinetics of faulting
432 in the leading Australian plate continental crust, which accommodates the effects of
433 non-orthogonal subduction. The distinctive faulting styles described include those
434 which could explain features on the T–E block (Cunningham & Anscombe 1985, Fig. 2)
435 by inverting the rotation effect of strike slip faulting on arcuate faults (Lamb 2011, Fig.
436 18 a), combined with dextral strike slip faulting on a curved strike slip fault “hinge”
437 (Lamb 2011, Fig. 18 f). Block rotation may be contemporaneous with or post-date
438 block formation. Block formation by ridge-traverse faults may have begun “long before
439 the block geometry became so prominent after Late Miocene time” (Scholl & Herzer
440 1994). Since the western margin of the T–E block has a down-to-Tofua NNE-SSW fault
441 pattern consistent with the other blocks, any rotation, as noted by Gatliff et al. (1994),
442 must have occurred before the ancestral Lau Tonga arc splitting commenced in the late
443 Late Miocene (5.3 Ma). An event at c. 10 Ma was detected by sediment backstripping
444 analysis on the Tonga Ridge at ODP 841 (Clift et al. 1994) and hence in the early Late

445 Miocene. We now propose a model by which block rotation may have contributed
446 towards the dispersal distance anomaly. The model crucially suggests that, pre-ancestral
447 Lau-Tonga Ridge splitting, a Middle Miocene volcano on what would become
448 subjacent Block A sourced the 'Eua accretionary lapilli found on what would become
449 Block T-E. Anticlockwise block rotation after deposition, but before Lau Basin opening
450 commenced in the late Late Miocene, affects Block T-E, but not A or N. After rotation
451 of this block, the Nomuka Group islands maintain their distance from source volcano,
452 but 'Eua has been displaced tectonically 40 km eastwards from the tephra source. The
453 distance between source and resting place for the accretionary lapilli has been increased
454 by 40 km even before ridge splitting in the latest Late Miocene carries 'Eua further east.
455

456 **Constraining dispersal distances for accretionary lapilli**

457 The evidence for final deposition of the 'Eua accretionary lapilli by settling through a
458 marine column of not less than 1600 meters, as presented in Cunningham & Beard
459 (2014), has been summarised earlier. The processes by which they could have reached
460 the point of settlement will now be reviewed. The present Tofua active volcanic arc
461 (Fig. 1B) is composed of emergent, barely emergent and submarine volcanic edifices at
462 modest depths and may be a good proxy for the Middle Miocene ancestral active
463 volcanic arc, given the dominantly volcanic insular geology as described earlier for the
464 remnant Lau Ridge. The ash clouds within which ash aggregates form (Brown et al.
465 2012) are typically associated with subaerial explosive volcanic eruptions, although
466 shallow marine eruptions can also be contenders if they breach water depths (McBirney
467 1963; Wright & Gamble 1999; White et al. 2003) with the creation of an atmospheric
468 ash cloud. The 'Eua accretionary lapilli may therefore have formed during an
469 explosive volcanic eruption initiated subaerially from an emergent volcanic edifice or at
470 shallow depths. In addition, proximity of the ocean surface permits the possibility of
471 formation of accretionary lapilli in secondary ash-rich steam clouds as pyroclastic
472 density currents enter the sea (Dufek et al. 2007). Dispersal may take place subaerially
473 within the eruption plume/umbrella cloud or as pyroclastic density currents travel across
474 the sea surface (Allen & Cas 2001; Carey et al. 1996; Maeno & Taniguchi 2007).
475 The 'Eua accretionary lapilli contain examples typically 10–15 mm in diameter and are
476 accretionary lapilli *sensu stricto* (Brown et al. 2010, Van Eaton & Wilson 2013), as
477 distinguished from less ordered ash pellets and fragile ash aggregates (Brazier et
478 al. 1982; Carey & Sigurdsson 1982; Wiesner et al. 1995; Brown et al. 2012) which rarely

Formatted: Pattern: Clear (White), Tab stops: 2", Left

479 ~~survive in that form but are detected in sieve analysis of grain size.~~—The substantial
 480 distances by which ~~less-ordered ash aggregates~~ can be dispersed from source
 481 subaerially are well established; ash aggregates dispersed in the eruption plume at Mt St
 482 Helens were detected at 200 km from source (Carey & Sigurdsson 1982). In contrast,
 483 the dispersal of relatively large and dense accretionary lapilli within the eruption plume
 484 must be restricted by their significant mass to more modest dispersal distances from the
 485 source volcano. ~~distances for accretionary lapilli *sensu stricto* of “a few to a few tens~~
 486 ~~of km” of Smellie (1984) accord with the intuition that dispersal of relatively large~~
 487 ~~spheroidal accretionary lapilli through the atmosphere must be restricted by their~~
 488 ~~significant mass to modest dispersal distances from the source volcano.~~ as constrained
 489 in tephra dispersal models (Walker et al. 1971; Walker 1981; Carey & Sparks 1986;
 490 Pfeiffer et al. 2005; Folch 2012). Accretionary lapilli are technically lapilli, falling
 491 within the 2–64 mm range. ~~Accretionary lapilli are technically lapilli, falling~~
 492 ~~within the 2–64 mm range of Schmid (1981; Fisher & Schmincke 1984) and “larger~~
 493 ~~centrimetric and millimetric fragments typically settle in minutes to a few hours at~~
 494 ~~distances of the order of tens of km from the volcano” (Folch 2012).~~ Lapilli-sized
 495 tephra can be dense juvenile/country rock clasts, mafic scoria or vesicular silicic pumice
 496 clasts. Reported specific gravities of accretionary lapilli, which are dominantly silicic,
 497 are in the range of 1200–1500 kg m⁻³ (Sparks et al. 1997). The 'Eua examples are mafic
 498 in composition and should therefore be at the upper end of this spectrum or slightly
 499 exceed it. Isopleths for 16 mm-sized lapilli for known eruptions show maximum
 500 dispersal distance in the range of 20–30 km (Carey & Sparks 1986), for tephra at
 501 density of 2500 kg m⁻³ and “larger centrimetric and millimetric fragments typically
 502 settle in minutes to few hours at distances of the order of tens of km from the volcano”
 503 (Folch 2012). Grain size directly influences terminal velocity of descent of a particle.
 504 This varies significantly with height in the atmosphere and departure from sphericity
 505 (Dellino et al. 2005). These parameters are accommodated in most tephra transport and
 506 dispersal models. Table 1 provides indicative terminal velocities over a range of heights
 507 (Pfeiffer et al. 2005) for particles of $\Phi = -4$ (=16 mm), density of 1500 kg m⁻³, and
 508 departure from sphericity. These particles are close to the typical size of the 'Eua
 509 accretionary lapilli. The density of 1500 kg m⁻³ is appropriate, as discussed earlier
 510 (advanced palagonitisation obscures the original density of the constituent glass
 511 particles). These figures would underestimate terminal velocity for the notably
 512 spheroidal 'Eua accretionary lapilli. The range of contemporary prevailing wind speeds

Formatted: Not Superscript/ Subscript

513 in the Lesser Antilles range from 5.55 m sec⁻¹ in the stratosphere and up to 25 m sec⁻¹ in
514 the upper troposphere (Sigurdsson et al.1980). Based on input of the 16 mm clast
515 isopleth for Cotopaxi layer 3, Burden et al. (2011) estimate plume height between 26
516 km and 32.5 km with a wind speed of 35 m sec⁻¹. If these wind speeds were applicable
517 to the SW Pacific in the Middle Miocene, the effects of wind advection should be
518 modest for tephra the size of the 'Eua accretionary lapilli. Complexity is introduced by
519 the formation of aggregates during plume development, whether in the form of
520 accretionary lapilli or less-ordered ash aggregates, as this is complex to model (Costa et
521 al. 2010); accretionary lapilli often occur in phreatomagmatic eruptions, where phase
522 changes involving latent heat release might increment the upwards convection vector
523 and counter the dominant role, in most models, of the downward terminal ("settling")
524 velocity of descent. Modelling of the phreatomagmatic 25.4 ka Oruanui event (Van
525 Eaton et al. 2012), an ultra-Plinian event, instead of a simple plume/high level umbrella
526 cloud with lower level co-ignimbrite ash clouds, produced "hybrid" ash clouds
527 generated both from the plume and from buoyant co-ignimbrite ash clouds which rise to
528 plume heights. Concentrically layered accretionary lapilli similar to those in 'Eua were
529 dispersed at distances of 120 km from source (Van Eaton & Wilson 2013) in this event.
530 The 25.4 ka Oruanui event is statistically unusual; only 156 (2.3 %) such events are
531 reported from a total of 6736 in the Smithsonian Institute database (Siebert and Simkin
532 2002–2014). Occurrences from more modest events are reported from dispersal within
533 the Soufriere St Vincent plume at 36 km from source (Brazier et al. 1982) and dispersed
534 within pyroclastic density currents at Mt St Helens at c. 25 km (Fisher et al. 1987), and
535 these are closer to ash pellets as defined (Brown et al 2010; Van Eaton & Wilson 2013),
536 rather than accretionary lapilli. The occurrence of layered accretionary lapilli at 'Eua
537 type are the same type as those dispersed at distances of 120 km from the 26.5 ka ultra-
538 Plinian Oruanui event (Van Eaton & Wilson 2013), are atypical under this view. In
539 contrast, occurrences associated with Soufriere St Vincent at 36 km from source
540 (Brazier et al. 1982) and with Mt St Helens at c. 25 km (Fisher et al. 1987) are potential
541 members of the typical "a few to a few tens of km" class, but these are closer to ash
542 pellets as defined, rather than accretionary lapilli.
543 The present Tofua active volcanic arc (Fig. 4) is composed of emergent, barely
544 emergent and submarine volcanic edifices at modest depths and may be a good proxy
545 for the Middle Miocene ancestral active volcanic arc, given the dominantly volcanic
546 insular geology as described earlier for the remnant Lau Ridge. Accretionary lapilli

547 normally form within atmospheric ash clouds associated with subaerial explosive
548 volcanic eruptions (Brown et al. 2012), although shallow marine eruptions can also be
549 contenders if they breach water depths (McBirney 1963; Wright & Gamble 1999; White
550 et al. 2003) with the creation of an atmospheric ash cloud. The 'Eua accretionary lapilli
551 may therefore have formed during an explosive volcanic eruption initiated subaerially
552 from an emergent volcanic edifice or at shallow depths. In addition, proximity of the
553 ocean surface permits the possibility of formation of accretionary lapilli in secondary
554 ash rich steam clouds as pyroclastic density currents enter the sea (Dufek et al. 2007).
555 Dispersal may therefore occur subaerially by expansion of the eruption plume,
556 spreading of any associated atmospheric umbrella cloud, and/or by associated
557 pyroclastic density currents, but these would rapidly encounter the sea. There is no
558 evidence for dispersal within submarine sediment gravity flows within the 'Eua
559 accretionary lapilli occurrences (Cunningham & Beard 2014); they appear to have
560 settled vertically under gravity. However, for accretionary lapilli dispersed within
561 pyroclastic density currents, surface dispersal over the ocean surface is now must be
562 considered. Pyroclastic density currents can partition into a coarse, dense-clast rich
563 submarine flow and a dilute pyroclastic surface flow -running at the surface on entering
564 the sea, as seen with experiments and simulations referred to observed/inferred events
565 and their deposits (Freundt 2003; Trofimovs et al. 2006; Dufek & Bergantz 2007;
566 Trofimovs et al. 2006; Trofimovs et al. 2008; Dufek et al. 2009). Such surface flows
567 have travelled for considerable distances (Allen & Cas 2001, Carey et al. 1996, Maeno
568 & Tanaguchi 2007) and carrying bombs and lapilli sized clasts, in addition to ash and
569 hot gas. Observations of the deposits of the Kos Plateau Tuff (Allen & Cas 2001)
570 supported this model, with the loss of the coarsest vent and conduit-derived lithic clasts
571 over the sea due to sinking, while over land, saltation was considered to have preserved
572 the coarser element in the resulting ignimbrites. Saltation may also occur over water and
573 be accentuated by the occurrence of pumice rafts (Fiske et al. 2001) while, conversely,
574 transport capacity will be influenced by areal dilution, as momentum transfer between
575 large and small particles is diminished (Dufek & Bergantz 2007; Dufek et al. 2009).
576 Such surface flows have travelled for considerable distances (Table 2), carrying bomb
577 and lapilli-sized clasts, in addition to ash and hot gas. Pyroclastic flows are more
578 common in silicic eruptions where juvenile volatiles are present, while those associated
579 with basaltic eruptions chiefly arise from phreatomagmatic activity (Yamamoto et al.

580 2005). The 'Eua tephra is heavily palagonitised, and surviving crystal mineralogy
581 suggests a basaltic andesite composition for the source (Cunningham and Beard 2014).

582

583 **Insights from tephra dispersal models for explosive volcanic eruptions**

584 Lapilli-sized tephra can be dense juvenile/country rock clasts, mafic scoria or vesicular
585 silicic pumice clasts. Reported specific gravities of accretionary lapilli, which are
586 dominantly silicic, are in the range of 1200–1500 kg m⁻³ (Sparks et al. 1997). The 'Eua
587 examples are mafic in composition and should therefore be at the upper end of this
588 spectrum or slightly exceed it. Tephra dispersal models could provide some insights for
589 dispersal of equivalently sized/dense accretionary lapilli. Isopleths for 16-mm-sized
590 lapilli for known eruptions show maximum dispersal distance in the range of 20–30 km
591 (Carey & Sparks 1986), for tephra at density of 2500 kg m⁻³. Such work constrained
592 dispersal within the plume (where the buoyant upwards vector and a downward terminal
593 velocity vector act on ash/tephra to form elast support envelopes, outside of which
594 particles descend vertically), and a lateral vector within the spreading umbrella cloud in
595 a wind-free environment, with any wind advection force further modifying dispersal
596 patterns. A full range of tephra dispersal models is now available (Foleh 2012).

597 However not only must the source be modelled and the atmosphere into which the
598 sourced particles are introduced but also, critically for this paper, a transport model
599 incorporated which can accommodate transformations during transport. Costa et al.
600 (2010) noted that “a complete description of ash aggregation in volcanic clouds is a very
601 arduous task and the full coupling of ash *transport* (our italics) and ash *aggregation*
602 *models* (our italics) is still computationally prohibitive”. Accretionary lapilli and lapilli
603 fundamentally differ in locus of formation; lapilli *sensu stricto* exist at eruption
604 inception, while the transformation represented by the formation of aggregates, whether
605 in the form of accretionary lapilli or the less-ordered ash aggregates referred to earlier,
606 takes place as the eruption cloud develops. Furthermore, early convection advection
607 models viewed the tephra being dispersed as passive in a dispersal process driven by
608 decompression of magmatic gases. Experimental work has established the key role of
609 vapour, liquid and solid phases of H₂O in the process of formation of accretionary lapilli
610 (Gilbert and Lane 1994, Schumacher and Schmincke 1995, Van Eaton et al. 2012 b).
611 Accretionary lapilli typically occur in phreatomagmatic eruptions, where phase changes
612 involving latent heat release might increment the upwards convection vector and
613 counter the dominant role, in most models, of the downward terminal (“settling”)

614 velocity of descent (Pfeiffer et al. 2005, Folch 2012). Hence the initial caution advised
 615 in applying such models where wet eruptions are involved (Carey & Sparks 1986). This
 616 caution is justified; the ATHAM model, forced with data from the phreatomagmatic
 617 26.5 ka Oruanui event, and run with $\geq 24\%$ H₂O relative to a MER of $1.1 \cdot 10^9$ kg (Van
 618 Eaton et al. 2012 a), instead of a simple plume/high level umbrella cloud with lower
 619 level co-ignimbrite ash clouds, produced “hybrid” ash clouds generated both from the
 620 plume and by buoyant co-ignimbrite ash clouds which rise to plume heights. This
 621 challenges simple distinctions between the plume/umbrella cloud and ash clouds related
 622 to pyroclastic density currents, both of which have a potential role in the formation and
 623 dispersal of accretionary lapilli.
 624 The 26.5 ka Oruanui event, an ultra-Plinian event, is statistically unusual; only 156 (2.3
 625 %) such events are reported from a total of 6736 in the Smithsonian Institute database
 626 (Siebert and Simkin 2002–2014).

627 **Dispersal by pyroclastic density currents travelling over the ocean surface**

628 An experimental approach (Freundt 2003) suggested that, on entering the sea,
 629 coarser/denser particles would continue flowing under water, while a dilute ash cloud
 630 would flow over the sea surface. Observations of the deposits of the Kos Plateau Tuff
 631 (Allen & Cas 2001) supported this model, with the loss of the coarsest vent and conduit-
 632 derived lithic clasts over the sea due to sinking, while over land, saltation over the water
 633 surface was considered to have preserved the coarser element in the resulting
 634 ignimbrites. Saltation may also occur over water and be accentuated by the occurrence
 635 of pumice rafts (Fiske et al. 2001) while, conversely, transport capacity will be
 636 influenced by dilution, as momentum transfer between large and small particles is
 637 diminished (Dufek & Bergantz 2007, Dufek et al. 2009). The actual extent of the
 638 contemporary sea surface has been challenged (Pe Piper et al. 2005) but in the area
 639 south of Kos, where dispersal of 39 km and possibly 60 km was reported (Table 1),
 640 there is support for the existence of a shallow sea surface (Dufek et al. 2009).

641

Event	DRE (km ³)	Largest Tephra (mm)	Distance from source (km)	Maximum distance (km)
Krakatoa	12	"small stone"	65	80
Kos Plateau Tuff Unit-D	10	50	35	>39

Unit E	30	200	35	>60
Koya Tuff	4			>40

642 In conclusion,

Formatted: Font: Not Bold

643 **Table 1** — Dispersal of larger tephra by pyroclastic density currents travelling over
644 the ocean surface, from Allen & Cas (2001), Carey et al. (1996). DRE = dense rock
645 equivalent. Maximum distance = maximum dispersal distance estimated for the event.

646
647 Accretionary lapilli only form when conditions within an ash cloud (whether Plinian or
648 those co-eval with pyroclastic density currents) are favourable and many explosive
649 eruptions do not produce them. No accretionary lapilli have been reported from the
650 Krakatoa 1883 eruption, despite their noted abundance in pyroclastic flow deposits
651 associated with silicic phreatomagmatic activity (Carey et al. 1996). Caution is
652 therefore required; the instances in Table 1 have reported the dispersal of lapilli by
653 pyroclastic density currents over the ocean surface, but not *accretionary* lapilli.
654 The major Krakatoan event delivered lapilli ("small stones") at 65 km and later mud
655 rain over a large area, associated with a climactic increase in magma discharge rate
656 leading to an increase of formation/delivery of pyroclastic flows into and over the sea,
657 rather than a phreatomagmatic phase of eruption initiated at the vent. Instead of magma-
658 water interaction at the vent, a complex, large, co-ignimbrite plume with strong
659 temperature and H₂O gradients is inferred to have been generated during dispersal over
660 land and sea. Increasing distance from source increased the H₂O content but buoyant
661 uplift of the hot core led to cooling and condensation, resulting in distal mud rain.
662 However little evidence was found to support the uptake of seawater in distal flows for
663 the Kos Plateau Tuff (Allen & Cas 2001). Variation in the degree of magma-water
664 interaction at the vent or uptake of H₂O during dispersal may contribute significantly to
665 dispersal distances; the maximum dispersal distance for the Koya Tuff suggests there is
666 no simple relation to the scale of the source eruption, certainly as measured by dense
667 rock equivalent (DRE).

669 **Scaling possible dispersal distances**

670 Other than the size of the accretionary lapilli and knowledge of current wind
671 directions/speeds at elevation, there is no data (e.g. isopleths from which the DRE may
672 be calculated) on the Middle Miocene eruption which supplied the 'Eua accretionary
673 lapilli. Hence no plume modelling of height attained and lateral dispersal within the
674 plume/spreading umbrella cloud is possible, even if the other difficulties discussed

675 above could be resolved. Grain size directly influences terminal velocity of descent of a
 676 particle. This varies significantly with height in the atmosphere and departure from
 677 sphericity (Dellino et al. 2005). These parameters are accommodated in most tephra
 678 transport and dispersal models. Table 2 provides indicative terminal velocities over a
 679 range of heights (Pfeiffer et al. 2005) for particles of $\phi = 4$ (16 mm), density of 1500
 680 kg m^{-3} , and a sphericity measure (F).

681

682

683

684

685

686

687 Height (km) ————— Sea level — 10 — 15 — 20 — 26

688 U_t (m sec^{-1}) ————— — 17 — 27 — 48 — 50 — 100

689

690 **Table 2**— Values for U_t , vertical terminal velocity at height, for particles of diameter
 691 16 mm, density of 1500 kg m^{-3} and F (sphericity) = 0.43, from Pfeiffer et al. (2005).

692

693 These particles are close to the typical size of the 'Eua accretionary lapilli. The density
 694 of 1500 kg m^{-3} is appropriate, as discussed earlier (advanced palagonitisation obscures
 695 the original density of the constituent glass particles). These figures would
 696 underestimate terminal velocity for the notably spheroidal 'Eua accretionary lapilli.

697 The effect of wind advection can be scaled by reference to these terminal velocity

698 calculations. The range of contemporary prevailing wind speeds in the Lesser Antilles
 699 range from 5.55 m sec^{-1} in the stratosphere and up to 25 m sec^{-1} in the upper troposphere
 700 (Sigurdsson et al. 1980). Based on input of the 16 mm clast isopleth for Cotopaxi layer

701 3, Burden et al. (2011) estimate plume height between 26 km and 32.5 km with a wind

702 speed of 35 m sec^{-1} . Hence, if these wind speeds are applicable to the SW Pacific,

703 terminal velocity of descent will significantly exceed wind speed. Unless dispersed

704 further laterally in the plume/umbrella cloud, lapilli of significant size (and hence mass)

705 should alight within distances significantly less than the maximum height at which they

706 commence descent. The jetstream could further accentuate dispersal. However 'Eua in

707 the Middle Miocene, pre Lau Basin opening, would still be at c. 20° S and hence some

708 distance from the contemporary jetstream path at 30–60°S, where wind speeds are
709 much higher (Bursik et al. 2009).
710 For plume/umbrella cloud dispersal within the atmosphere, lateral wind advection
711 should be modest for these particles of significant mass; the "few to a few tens of km"
712 metric is supported. intuition seems to have some scientific basis. For pyroclastic
713 density current-enabled dispersal over land, only a statistically unlikely ultra-Plinian
714 event is capable of providing dispersal via the atmosphere for the minimum 70 km
715 dispersal scenario, (considering the source was close to the eastern edge of the remnant
716 Lau Ridge segment). In contrast, for pyroclastic density current-enabled dispersal
717 across the ocean surface, there is some evidence that relatively modest magnitude
718 events could provide dispersal distances which contribute significantly to the
719 scenario. this figure.

720

721

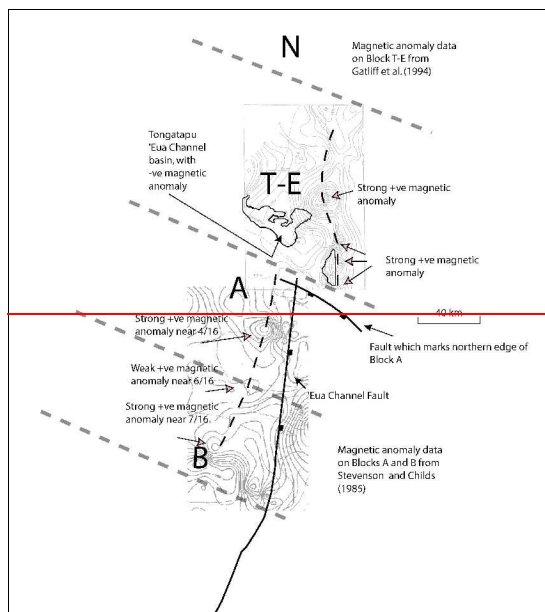
722 **Block rotation; the Tongatapu–Eua block**

723 During re-processing of oil industry data on the T–E Block, it was noted that a number
724 of physiographic features of the block would be explained if it had rotated 30°
725 anticlockwise (Gatliff et al. 1994). One characteristic is the atypical triangular shape of
726 the Tongatapu–Eua block as a whole (Fig. 4), as reflected at the 1000 m isobath. Eua
727 is closer to the eastern margin of the frontal arc basin than any other basement high and
728 as an emergent island with an elevation of 912 meters, is much higher. To further
729 explore whether there is seismostratigraphic/geophysical support for the rotation
730 proposition, a number of sources of data were superimposed on Blocks A, B and T–E
731 (Fig. 8).

732

733

734



735

736

737 **Figure 8.**—Discontinuity of trends across the boundary between tectonic Blocks A, B
738 and T-E.

739

740 There are clearly a number of departures from the Tonga Ridge NNE-SSW ridge-
741 parallel structural trend, localised to the southern margin of Block T-E. The departures
742 are:

743

744 1. — On Block T-E, a trend in magnetic intensity anomalies, broadly coincident with
745 gravity/are basement highs (Gatliff et al. 1994) departs from trend and is deflected east
746 of 'Eua;

747

748 2. — Further south, on Blocks A and B, a trend of magnetic intensity anomalies
749 (Stevenson & Childs 1985), coincident with ridge-parallel are basement highs, is
750 abruptly curtailed as the southern margin of the T-E block is encountered.

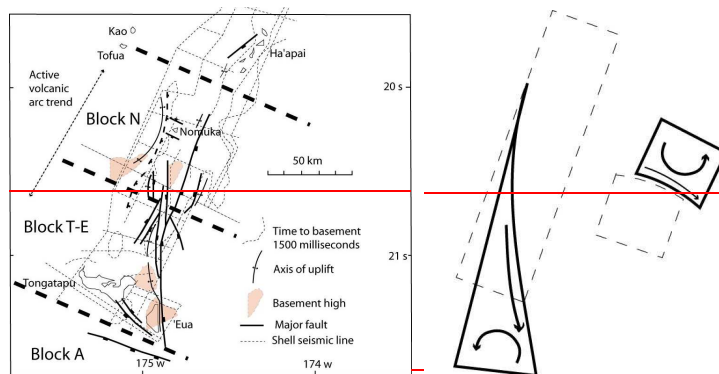
751

752 3. — The 'Eua Channel Fault, a major structural feature on the southern Tonga Ridge
753 disappears north of the block margin, where a magnetic intensity low centred on
754 Tongatapu/the 'Eua Channel was identified as a sedimentary basin which shallowed to
the east and north (Gatliff et al. 1994).

754

755 The three positive magnetic intensity highs immediately east of 'Eua on the Tongatapu
 756 'Eua block appear to be displaced by a strike-slip fault c. 40 km to the east of the trend
 757 of the magnetic intensity highs on Blocks A and B. This would have the effect of
 758 anticlockwise rotation *sensu* Gatliff et al. (1994). The southern margin of Block T-E is
 759 perhaps better considered as a fault zone than localised on one fault. On the T-E block a
 760 horst runs NW-SE into Tongatapu (Fig. 9) and this trend is seen onshore on 'Eua, where
 761 faults dominantly trending NW-SE cut the Middle Miocene volcanoclastics and show
 762 evidence of lateral movement (Lowe 1987). North of 'Eua, these trends are restored to
 763 ridge-parallel orientation.

764



765

766

767 **Figure 9.** — Left: basement trends and faults on Blocks A, T-E and N, after
 768 Cunningham & Ancombe (1985). Right: rotation effect of strike-slip faulting on
 769 areuate faults, accommodated by strike-slip faulting on a curved fault “hinge”, after
 770 Lamb (2011).—

771

772 Further south on the Tonga-Kermadec-Hikurangi trend, Lamb (2011) reviews the
 773 tectonics and kinematics of block faulting in the leading Australian plate continental crust,
 774 which accommodates the effects of non-orthogonal subduction. A number of
 775 distinctive block faulting styles are detected, one of which appears to be expressed on
 776 the T-E block (Fig. 9) where the anticlockwise rotation effect of sinistral strike-slip
 777 faulting on areuate faults is accommodated by dextral strike-slip faulting on a curved
 778 strike-slip fault “hinge”.

779

780 **Timing of block formation and rotation**

781 Block rotation may be contemporaneous with or post-date block formation.

782 Block formation by ridge-traverse faults may have begun “long before the block

Formatted: Pattern: Clear (White)

783 geometry became so prominent after Late Miocene time" (Scholl & Herzer 1994 and
784 Supplementary File A). Since the western margin of the T-E block has a down to Tofua
785 NNE-SSW fault pattern consistent with the other blocks, any rotation, as noted by
786 Gatliff et al. (1994), must have occurred before the ancestral Lau-Tonga are splitting
787 commenced in the late Late Miocene (5.25 Ma).

788 The Tonga Ridge strikes c. N 20° E. The mean azimuth of slip vectors along the Tonga
789 trench from 35–19° S ranges from N280° E' to N285° E' (Pelletier & Louat 1989). If this
790 applied in the Middle Miocene, prior to the ancestral c. north-trending Lau/Tonga
791 Ridge splitting, non-orthogonal subduction would then have imparted a lateral vector to
792 regional stress patterns, thus providing a similar environment to that associated with
793 block rotation in leading edge continental crust further south on the Tonga-Kermadec-
794 Hikurangi trend. An event at c. 10 Ma was detected by sediment backstripping analysis
795 on the Tonga Ridge at ODP 841 (Clift et al. 1994) and hence in the early Late Miocene.
796 In conclusion, the data provides some support for the provision by block rotation of a
797 right-lateral strike-slip movement of c. 40 km in a fault zone centred on the south of
798 Block T-E and the north of Block A area, after 14 Ma and before splitting of the
799 ancestral Lau/Tonga Ridge commenced in latest Late Miocene. A model is now
800 proposed by which block rotation may have contributed towards the dispersal distance
801 anomaly. The model crucially suggests that, pre-ancestral Lau-Tonga Ridge splitting, a
802 Middle Miocene volcano on what would become subadjacent Block A sourced the 'Eua
803 accretionary lapilli found on what would become Block T-E. Anticlockwise block
804 rotation after deposition, but before Lau Basin opening commenced in the late Late
805 Miocene (5.25 Ma), affects Block T-E, but not A or N. After rotation of this block, the
806 Nomuka Group islands maintain their distance from source volcano, but 'Eua has been
807 displaced tectonically 40 km eastwards from the tephra source. The distance between
808 source and resting place for the accretionary lapilli has been increased by 40 km even
809 before ridge splitting in the latest Late Miocene carries 'Eua further east.

811 Discussion and conclusions

812 The accretionary lapilli on 'Eua, Tonga, occur in Middle Miocene pelagic volcanoclastic
813 sediments with no compelling evidence for a proximal volcanic source. A
814 contemporary distance which is unlikely to be less than 70 km, and may be much more,
815 from a source on the Lau segment of the ancestral Lau-Tonga Ridge, is estimated from
816 seismostratigraphic and other data. This distance is much further than would be

Formatted: Tab stops: 5.25", Left

817 expected for dispersal of these spheroids of significant mass, unless an exceptional
 818 ultra-Plinian source is invoked. ~~'Eua is positioned much further from the western edge~~
 819 ~~of the Tonga Ridge than any other island and hence much further from a western Lau-~~
 820 ~~Tonga ancestral arc volcanic source. Tephra fall associated with Aa~~ an ultra-Plinian
 821 event on the scale of the Oruanui at ~~25.46.5~~ 25.46.5 ka (Van Eaton & Wilson 2013) could,
 822 *prima facie*, resolve the dispersal distance problem, since the dispersal distances of
 823 accretionary lapilli ~~in the atmosphere by the eruption plume and pyroclastic density~~
 824 ~~currents~~ in that event were substantial. ~~layered accretionary lapilli, the type reported~~
 825 ~~from 'Eua (Cunningham & Beard 2014), with diameters sometimes in excess of 10 mm~~
 826 ~~occur up to 120 km from the virtual source at Lake Taupo.~~ However, there is no field
 827 evidence in the area under study for an ultra-Plinian event in the Middle Miocene. At
 828 530 km³ DRE, the Oruanui event is exceptional and unit 8, which contains the highly
 829 dispersed occurrences, exhibits characteristics which suggest that the eruption produced
 830 an extremely high mass eruption rate ($\geq 10^9$ kg s⁻¹), with numerical simulations (Van
 831 Eaton et al. 2012a) implying the potential for transportation of tephra to stratospheric
 832 heights. Explosive volcanic events of a much more modest ~~magnitude~~ DRE, but driving
 833 pyroclastic density currents over the ocean surface, have dispersed tephra to
 834 considerable distances (Table 2), with ~~"small stones"~~ larger tephra being carried as far
 835 as 65 km. ~~The~~ The transportation of large vent- and conduit derived clasts (with
 836 densities as high as 2500 kg m⁻³) during transport of the Kos Plateau Tuff across the
 837 ocean for considerable distances supports the credibility of dispersal by this process.
 838 The restriction of upper size carried, depending on mass flux during the individual
 839 event, ~~units, also has local~~ has significance for the Tongan insular Miocene, on 'Eua,
 840 where the absence of clasts exceeding 320 mm has been attributed to some trapping
 841 mechanism elsewhere (Ballance et al. 2004) for clasts of greater size. Delivery by
 842 sediment gravity flows is probable for most of the volcanoclastics on the 'Eua high
 843 (Tappin & Ballance 1994; Ballance et al. 2004). However, for any component of the
 844 'Eua volcanoclastics delivered by ocean surface pyroclastic density currents, rather than
 845 by sediment gravity flows, an alternative alternative process by which upper grain size
 846 is restricted is suggested by the Kos Plateau Tuff event. Furthermore, the rare
 847 westwards-dipping ~~had~~ cross-beds in the 'Eua volcanoclastics (Fig. 26D) may be
 848 attributable to sediment overloading on the 'Eua high by periodic ocean surface
 849 pyroclastic density currents and consequential westwards backflow.
 850 While delivery by pyroclastic density current over the ocean surface may explain all or

Formatted: Font: Italic

Formatted: Superscript

851 part of the dispersal distance issue, it does not explain the anomalous position of the
852 'Eua high; ~~'Eua is positioned much further from the western edge of the Tonga Ridge~~
853 ~~than any other island.~~ The discontinuities in trends at the southern Block T–E margin,
854 interpreted as block rotation of a particular type, provides a tectonic explanation for this
855 anomaly. The relative thickness of sediment in the Tongatapu/'Eua Channel depocentre
856 (Fig. 48) fits well within this model; with block rotation occurring in the Late
857 Miocene, but pre-splitting, the Tongatapu—'Eua Channel basin would have been 40
858 km closer to the source volcanoes to the west for part of the interval 14 – 5.253 Ma,
859 ~~thus only 30 km from source on the minimum 70 km scenario.~~
860 ~~For~~ the rotation event ~~may also to~~ have contributed 40 km to the 'Eua accretionary
861 lapilli dispersal distance, ~~subject~~ a number of conditions must apply. Firstly it must pre-
862 date splitting of the ancestral Lau/Tonga Ridge which commenced in latest Late
863 Miocene (5.325 Ma), secondly post-date the deposition of the accretionary lapilli on
864 proto-'Eua at 14 Ma, and thirdly, the accretionary lapilli must have been sourced from a
865 volcano on the ancestral Lau-Tonga Ridge segment which became Block A.
866 We favour a model where ~~the~~ accretionary lapilli on 'Eua finally settled through a
867 marine column of not less than 1600 meters. Their delivery to the final resting
868 ~~settlement~~ site was most likely achieved by transport within a pyroclastic density
869 current travelling over the ocean surface which, even in the case of those initiated by
870 small/moderate explosive volcanic events, have delivered relatively large tephra
871 considerable distances from source. ~~A~~ dual model, comprising block rotation and
872 dispersal by ocean surface pyroclastic density currents, can explain the anomalies
873 described and accommodate a large range of possible dispersal distances from a source
874 of modest ~~DRE~~ magnitude. ~~The possibility of dispersal within the hybrid ash cloud of an~~
875 ~~ultra-Plinian event of the Oruanui type is not excluded, but is not supported by any data.~~
876 ~~The~~ dating of block formation and of subsequent movement is however problematic;
877 ridge-normal faulting is only strongly expressed in displacement of the A–B isopach,
878 implying that it ~~occurred mostly p~~ postdated late Late Miocene. Only detailed
879 palaeomagnetic studies of the host Middle Miocene volcanoclastics on 'Eua could
880 increase precision in this regard; the ubiquity of magnetite in thin hemipelagites which
881 occur in these rocks would make such studies worthwhile.

882

883 **Acknowledgements**

884

885 JKC acknowledges the many in Tonga and on 'Eua who assisted during 2 years spent
886 there and during more recent visits. Funding from the UK Overseas Development

887 Agency and Birkbeck College supported the fieldwork. Shell International kindly
 888 provided copies of data sheets and their final report. Discussion, help and
 889 encouragement from Peter Ballance was crucial in framing the objectives of this paper.
 890 Subsequent assistance from Rick Hoblitt, Sharon Allen, Ben Ellis and Alexa Van Eaton
 891 greatly improved the execution. The detailed review points of Martin Jutzeler and an
 892 anonymous reviewer were crucial in achieving the final draft. The editors are thanked
 893 for their support.

894
 895 **Supplementary information published online**

896
 897 ~~Supplementary File 1: A more detailed summary of Tonga Ridge issues relevant to the~~
 898 ~~paper, supported by 7 figures and additional references.~~

899
 900 ~~Supplementary File 2: A more detailed summary on Lau Ridge issues relevant to the~~
 901 ~~paper, supported by a summary figure.~~

902
 903
 904
 905
 906
 907 **References**

908
 909 Alexander, C 1985. 2-D gravity and magnetic modelling of subsurface domical
 910 structure 11/14: Volcanic episodes in 'Eua, Tonga. In: Scholl DW, Vallier TL eds.
 911 Geology and Offshore Resources of Pacific Island Arcs—Tonga Region. [Earth Science](#)
 912 [Series 2. Houston, Texas](#), Circum-Pacific Council for Energy and Mineral Resources
 913 [Earth Science Series 2](#), Pp. 197–202.

914
 915 Allen SR, Cas RAF 2001. Transport of pyroclastic flows across the sea during the
 916 explosive rhyolitic eruption of the Kos Plateau Tuff, Greece. *Bulletin of Volcanology*
 917 62(6–7): 441–456.

918
 919 Austin J, Taylor FW, Cagle CD 1989. Seismic stratigraphy of the central Tonga Ridge.
 920 *Marine and Petroleum Geology* 6: 71–92.

921
 922 Ballance PF, Tappin DR, Wilkinson IP 2004. Volcaniclastic gravity flow sedimentation
 923 on a frontal arc platform: the Miocene of Tonga. *New Zealand Journal of Geology and*
 924 *Geophysics* 47: 567–587.

925
 926 Brazier S, Davis AN, Sigurdsson H, Sparks RSJ 1982. Fall-out and deposition of
 927 volcanic ash during the 1979 explosive eruption of the Soufriere of St. Vincent. *Journal*
 928 *of Volcanology and Geothermal Research* 14: 335–359.

929
 930 Brown RJ, Branney MJ, Maher C, Harris PD 2010. Origin of accretionary lapilli within
 931 ground-hugging density currents: evidence from pyroclastic couplets on Tenerife.
 932 *Bulletin of the Geological Society of America* 122: 305–320.

933
 934 Brown RJ, Bonadonna C, Durant AJ 2012. A review of volcanic ash aggregation.
 935 *Physics and Chemistry of the Earth* 45–46: 65–78.

936

Formatted: Font color: Black

- 937 [Burden RE, Phillips JC, Hincks TK 2011. Estimating volcanic plume heights from](#)
 938 [depositional clast size. Journal of Geophysical Research—Solid Earth, 116, No. B11,](#)
 939 [B11206, 20111116: B11206.](#)
- 940 [Burden RE, Phillips JC, Hincks TK 2011. Estimating volcanic plume heights from](#)
 941 [depositional clast size. Journal of Geophysical Research 116: B11206.](#)
 942 [doi:10.1029/2011JB008548.](#)
- 943
- 944 [Bursik MI, Kobs SE, Burns A, Braitseva OA et al. 2009. Volcanic plumes and wind:](#)
 945 [Jetstream interaction examples and implications for air traffic. Journal of Volcanology](#)
 946 [and Geothermal Research 186: 60–67.](#)
- 947
- 948 Carey SN, Sigurdsson H 1982. Influence of particle aggregation on deposition of
 949 distal tephra from the May 18, 1980, eruption of Mount St. Helens volcano. Journal of
 950 Geophysical Research 87: 7061–7072.
- 951
- 952 Carey SN, Sparks RSJ 1986. Quantitative models of the fallout and dispersal of tephra
 953 from volcanic eruption columns. Bulletin of Volcanology 48: 109–125.
- 954
- 955 Carey SN, Sigurdsson H, Mandeville C, Bronto S 1996. Pyroclastic flows and surges
 956 over water: an example from the 1883 Krakatau eruption. Bulletin of Volcanology 57:
 957 493–511.
- 958
- 959 Chaproniere GCH 1994. Middle and Late Eocene, Neogene, and Quaternary
 960 foraminiferal faunas from 'Eua and Vava'u Islands, Tonga group, In: Stevenson AJ,
 961 Herzer RH, Ballance PF eds. Geology and Submarine Resources of the Tonga-Lau-Fiji
 962 Region. SOPAC Technical Bulletin 8, [Suva, Fiji, South Pacific Applied Geoscience](#)
 963 [Commission. Pp. 21–44.](#)
- 964
- 965 Chase TE 1985. Submarine topography of the Tonga-Fiji Region and the southern
 966 Tonga platform area. In: [Scholl DW, Vallier TL eds. Geology and Offshore Resources](#)
 967 [of Pacific Island Arcs—Tonga Region. Circum-Pacific Council for Energy and Mineral](#)
 968 [Resources Earth Science Series 2, In: Scholl DW, Vallier TL eds. Geology and](#)
 969 [Offshore Resources of Pacific Island Arcs—Tonga Region. Earth Science Series 2,](#)
 970 [Houston, Texas, Circum-Pacific Council for Energy and Mineral Resources. Pp. 21.](#)
- 971
- 972 Clift PD, [Bednarz UB](#), Bøe R, [Bednarz UB](#) et al. 1994. Sedimentation on the Tonga
 973 forearc related to arc rifting, subduction erosion, and ridge collision: a synthesis of
 974 results from sites 840 and 841. In: Hawkins JW, Parson LM, Allan JF eds. Proceedings
 975 of the Ocean Drilling Program, [Scientific Results, Vol. 135](#)~~Scientific Results, 135,~~
 976 [College Station, Texas.](#) Pp. 843–873.
- 977
- 978 Clift PD and ODP Leg 135 Scientific Party 1995. Volcanism and sedimentation in a
 979 rifting island arc terrain: an example from Tonga, SW Pacific. In: Smellie JL ed.
 980 Volcanism associated with extension at consuming plate margins. Geological Society of
 981 London, Special Publication 88, Pp. 29–52.
- 982
- 983 Clift PD, McCleod CJ, Tappin DR, Wright DJ, Bloomer SH 1998. Tectonic controls on
 984 sedimentation and diagenesis in the Tonga Trench and forearc, southwest Pacific.
 985 Geological Society of America Bulletin 110: 483–496.
- 986

Formatted: Don't adjust space between Latin and Asian text, Don't adjust space between Asian text and numbers, Pattern: Clear

Formatted: Font: Times New Roman, 12 pt

Formatted: Font: Times New Roman, 12 pt

Formatted: Font: Times New Roman, 12 pt

Formatted: Font: Times New Roman, 12 pt

Formatted: Font: Times New Roman, 12 pt

Formatted: Font: Times New Roman, 12 pt

Formatted: Font: Times New Roman, 12 pt

- 987 Cole JW, Gill JB, Woodhall D 1985. Petrological history of the Lau Ridge, Fiji. ~~In:~~
 988 ~~Scholl DW, Vallier TL eds. Geology and Offshore Resources of Pacific Island Arcs–~~
 989 ~~Tonga Region. Circum-Pacific Council for Energy and Mineral Resources Earth~~
 990 ~~Science Series 2. In: Scholl DW, Vallier TL eds. Geology and Offshore Resources of~~
 991 ~~Pacific Island Arcs–Tonga Region. Earth Science Series 2. Houston, Texas, Circum-~~
 992 ~~Pacific Council for Energy and Mineral Resources. Pp. 379–391.~~
 993
 994 Costa A, Folch A, Macedonio G, Durant A. 2010. Modelling transport and aggregation
 995 of volcanic ash particles. EGU General Assembly 2–7 May 2010, Vienna, Austria.
 996 8965.
 997
 998 ~~Cunningham JK, Beard AD 2014. An unusual occurrence of mafic accretionary lapilli~~
 999 ~~in deep-marine volcanoclastics on 'Eua, Tonga: palaeoenvironment and process. Journal~~
 1000 ~~of Volcanology and Geothermal Research 274: 139–151.~~
 1001
 1002 Cunningham JK, Anscombe KJ 1985. Geology of 'Eua and other islands, Kingdom of
 1003 Tonga. ~~In: Scholl DW, Vallier TL eds. Geology and Offshore Resources of Pacific~~
 1004 ~~Island Arcs–Tonga Region. Circum-Pacific Council for Energy and Mineral Resources~~
 1005 ~~Earth Science Series 2 In: Scholl DW, Vallier TL eds. Geology and Offshore Resources~~
 1006 ~~of Pacific Island Arcs–Tonga Region. Earth Science Series 2. Houston, Texas, Circum-~~
 1007 ~~Pacific Council for Energy and Mineral Resources. Pp. 221–257.~~
 1008
 1009 ~~Cunningham JK, Beard AD 2014. An unusual occurrence of mafic accretionary lapilli~~
 1010 ~~in deep-marine volcanoclastics on 'Eua, Tonga: palaeoenvironment and process. Journal~~
 1011 ~~of Volcanology and Geothermal Research 274: 139–151.~~
 1012
 1013 ~~Dellino P, Mele D, Bonasia R, Braia G, La Volpe L, Sulpizio R 2005. The analysis of the~~
 1014 ~~influence of pumice shape on its terminal velocity. Geophysical Research Letters, 32:~~
 1015 ~~L21306. doi:10.1029/2005GL023954.~~
 1016
 1017 Dufek J, Bergantz GW 2007. Dynamics and deposits generated by the Kos Plateau Tuff
 1018 eruption: Controls of basal particle loss on pyroclastic flow transport. Geochemistry
 1019 Geophysics Geosystems 8, Q12. doi:10.1029/2007GC001741.
 1020
 1021 Dufek J, Manga M, Staedter M 2007. Littoral blasts: Pumice-water heat transfer and
 1022 the conditions for steam explosions when pyroclastic flows enter the ocean. Journal of
 1023 Geophysical Research 112, B11201. doi:10.1029/2006JB004910.
 1024
 1025 Dufek J, Wexler J, Manga M 2009. Transport capacity of pyroclastic density currents:
 1026 Experiments and models of substrate-flow interaction. Journal of Geophysical Research
 1027 114: B11203. doi:10.1029/2008JB006216.
 1028
 1029 Fisher RV, Glicken H, Hoblitt RP 1987. May 18, 1980, Mount St. Helens Deposits in
 1030 South Coldwater Creek, Washington. Journal of Geophysical Research - Solid Earth 92-
 1031 (B10): 10267–10283.
 1032
 1033 ~~Fisher RV, Schmincke H-U 1984. Pyroclastic rocks. Berlin, Springer-Verlag. 472 p.~~
 1034
 1035 ~~Fiske RS, Cashman, KV, Shibata, A, Watanabe K 1998. Tephra dispersal from~~
 1036 ~~Myojinsho, Japan, during its shallow submarine eruption of 1952–1953: Bulletin of~~
 1037 ~~Volcanology 59: 262–275.~~
 1038

Formatted: Don't adjust space between Latin and Asian text, Don't adjust space between Asian text and numbers

Formatted: Font: Times New Roman, 12 pt, Font color: Black, Spanish (International Sort)

Formatted: Font: Times New Roman, 12 pt, Font color: Black

Formatted: Font: Times New Roman, 12 pt, Font color: Black, Spanish (International Sort)

Formatted: Font: Times New Roman, 12 pt, Font color: Black

Formatted: Font: Times New Roman, 12 pt, Font color: Black, Spanish (International Sort)

Formatted: Font: Times New Roman, 12 pt, Font color: Black

Formatted: Font: Times New Roman, 12 pt, Font color: Black, Spanish (International Sort)

Formatted: Font: Times New Roman, 12 pt, Font color: Black

Formatted: Font: Times New Roman, 12 pt, Font color: Black, Spanish (International Sort)

Formatted: Font: Times New Roman, 12 pt, Font color: Black

Formatted: Font: Times New Roman, 12 pt, Font color: Black, Spanish (International Sort)

Formatted: Font: Times New Roman, 12 pt, Font color: Black

Formatted: Font: Times New Roman, 12 pt, Font color: Black, Spanish (International Sort)

Formatted: Font: Times New Roman, 12 pt, Font color: Black

Formatted: Font: Times New Roman, 12 pt, Font color: Black, Spanish (International Sort)

Formatted: Font: Times New Roman, 12 pt, Font color: Black

Formatted: Font: Times New Roman, 12 pt, Font color: Black, English (U.K.)

Formatted: English (U.K.)

- 1039 Folch A 2012. A review of tephra transport and dispersal models: Evolution, current
1040 status, and future perspectives. *Journal of Volcanology and Geothermal Research* 235–
1041 236: 96–115.
- 1042
- 1043 Freundt A 2003. Entrance of hot pyroclastic flows into the sea: experimental
1044 observations. *Bulletin of Volcanology* 65: 144–164. ~~doi:DOI~~ [10.1007/s00445-002-
1045 0250-1](https://doi.org/10.1007/s00445-002-0250-1).
- 1046
- 1047 Gatliff RW, Pflueger JC, Havard KR, Helu SP 1994. Structure, seismic stratigraphy and
1048 petroleum potential of the Tongatapu -Eua area of the Kingdom of Tonga. ~~In:~~
1049 ~~Stevenson AJ, Herzer RH, Ballance PF eds. *Geology and Submarine Resources of the*~~
1050 ~~*Tonga-Lau-Fiji Region. SOPAC Technical Bulletin 8*, In: Stevenson AJ, Herzer RH,~~
1051 ~~Ballance PF eds. *Geology and Submarine Resources of the Tonga-Lau-Fiji Region.*~~
1052 ~~*SOPAC Technical Bulletin 8. Suva, Fiji, South Pacific Applied Geoscience*~~
1053 ~~*Commission*. Pp. 107–119.~~
- 1054
- 1055 ~~▲~~ ~~Gilbert JS, Lane SJ 1994. The origin of accretionary lapilli. *Bulletin of Volcanology* 56:~~
1056 ~~398–411.~~
- 1057
- 1058
- 1059 Herzer RH, Exon NF 1985. Structure and basin analysis of the southern Tonga forearc.
1060 ~~In: Scholl DW, Vallier TL eds. *Geology and Offshore Resources of Pacific Island Arcs*~~
1061 ~~*-Tonga Region. Circum-Pacific Council for Energy and Mineral Resources Earth*~~
1062 ~~*Science Series 2*, In: Scholl DW, Vallier TL eds. *Geology and Offshore Resources of*~~
1063 ~~*Pacific Island Arcs-Tonga Region. Earth Science Series 2. Houston, Texas, Circum-*~~
1064 ~~*Pacific Council for Energy and Mineral Resources*. Pp. 55–74.~~
- 1065
- 1066 ~~*IAGA Division 1 Study Group 1976. International geomagnetic reference field 1965.*~~
1067 ~~*Journal of Geophysical Research* 74: 4407–4408.~~
- 1068
- 1069 Lamb S 2011. Cenozoic tectonic evolution of the New Zealand plate-boundary zone: A
1070 paleomagnetic perspective. *Tectonophysics* 509: 135–164.
- 1071
- 1072 ~~Lehner P, Doust H, Bakker G, Allenbach P, Guenne J 1983. Active margins, Part 2—~~
1073 ~~Tonga trench, profiles P-1200 and G-150. In: Bally AW ed. *Seismic expression of*~~
1074 ~~*structural styles. American Association of Petroleum Geologists. Studies in Geology*~~
1075 ~~*Series 15, Pp. 3.4.2 19–3.4.2 44.*~~
- 1076
- 1077 ~~Lowe, D.J., 1987. *Eua Island, Tonga, 1987 Expedition Report.*~~
1078 ~~Maeno F, Taniguchi H 2007. Spatiotemporal evolution of a marine caldera-forming~~
1079 ~~eruption generating a low-aspect ratio pyroclastic flow, 7.3 ka, Kikai caldera,~~
1080 ~~Japan: Implication from near-vent eruptive deposits. *Journal of Volcanology and*~~
1081 ~~*Geothermal Research* 167: 212–238.~~
- 1082
- 1083 McBirney AR 1963. Factors governing the nature of submarine volcanism. *Bulletin of*
1084 *Volcanology* 26 (Pt. 2): 455–469.
- 1085
- 1086 Packham, G.H., 1978. Evolution of a simple island arc: The Lau-Tonga Ridge.
1087 *Bulletin of the Australian Society of Exploration Geophysicists* 9: 133–140.
- 1088

Formatted: Font color: Black

Formatted: Font color: Red

Formatted: Font color: Black

Formatted: Font color: Black

- 1089 Parson LM, Rothwell RG, MacLeod CJ 1994. Tectonics and sedimentation in the Lau
 1090 Basin (southwest Pacific). In: [Hawkins JW, Parson LM, Allan JF eds. Proceedings of](#)
 1091 [the Ocean Drilling Program, Scientific Results, 135, . In: Hawkins JW, Parson LM,](#)
 1092 [Allan JF eds. Proceedings of the Ocean Drilling Program, Scientific Results, Vol. 135,](#)
 1093 [College Station, Texas.](#) Pp. 9–22.
- 1094
 1095 Parson LM, Wright IC 1996. The Lau-Havre-Taupo back-arc basin: A
 1096 southward-propagating, multi-stage evolution from rifting to spreading.
 1097 Tectonophysics 263: 1–22.
- 1098
 1099 ~~Pelletier B, Louat R 1989. Seismotectonics and present-day relative plate motions in
 1100 the Tonga-Lau and Kermadec-Havre region. Tectonophysics, 165, 237–250.~~
- 1101
 1102 ~~Pe-Piper G, Piper DJW, Perissoratis C 2005. Neotectonics and the Kos Plateau Tuff
 1103 eruption of 161 ka, South Aegean arc. Journal of Volcanology and Geothermal
 1104 Research 139, 315–338, doi:10.1016/j.jvolgeores.2004.08.014.~~
- 1105
 1106 Pfeiffer T, Costa A, Macedonio G 2005. A model for the numerical simulation of
 1107 tephra deposits. Journal of Volcanology and Geothermal Research 140: 273–294.
- 1108
 1109 Pflueger JC, Havard KR 1994. A re-examination of the line 11/14 anomaly on the
 1110 Southern Tonga Platform. In: [Stevenson AJ, Herzer RH, Ballance PF eds. Geology and](#)
 1111 [Submarine Resources of the Tonga-Lau-Fiji Region. SOPAC Technical Bulletin 8, In:](#)
 1112 [Stevenson AJ, Herzer RH, Ballance PF eds. Geology and Submarine Resources of the](#)
 1113 [Tonga-Lau-Fiji Region. SOPAC Technical Bulletin 8. Suva, Fiji, South Pacific Applied](#)
 1114 [Geoscience Commission.](#) Pp. 107–119.
- 1115
 1116 Quinterno PJ 1985. Cenozoic planktonic foraminifers and coccoliths from 'Eua,
 1117 Tongatapu and Nomuka Islands, southwest Pacific Ocean. In: [Scholl DW, Vallier TL](#)
 1118 [eds. Geology and Offshore Resources of Pacific Island Arcs—Tonga Region. Circum-](#)
 1119 [Pacific Council for Energy and Mineral Resources Earth Science Series 2, In: Scholl](#)
 1120 [DW, Vallier TL eds. Geology and Offshore Resources of Pacific Island Arcs—Tonga](#)
 1121 [Region. Earth Science Series 2. Houston, Texas, Circum-Pacific Council for Energy](#)
 1122 [and Mineral Resources.](#) Pp. 259–267.
- 1123
 1124 Sager WW, MacLeod CJ, Abrahamsen N 1994. Palaeomagnetic constraints on Tonga
 1125 Arc tectonic rotation from sediments drilled at Sites 840 and 841. In: [Hawkins JW,](#)
 1126 [Parson LM, Allan JF eds. Proceedings of the Ocean Drilling Program, Scientific](#)
 1127 [Results, 135, In: Hawkins JW, Parson LM, Allan JF eds. Proceedings of the Ocean](#)
 1128 [Drilling Program, Scientific Results, Vol. 135. College Station, Texas.](#) Pp.763–783.
- 1129
 1130 Schmid R 1981. Descriptive nomenclature and classification of pyroclastic deposits and
 1131 fragments: Recommendations of the International Union of Geological Sciences
 1132 Subcommission on the Systematics of Igneous Rocks. The Geological Society of
 1133 America, Boulder, Colorado. Volume 9, Pp. 41–43.
- 1134
 1135 Scholl DW, Vallier TL eds. 1985. Geology and offshore resources of the Pacific island
 1136 arcs—Tonga region. [Earth Science Series 2. Houston, Texas,](#) Circum-Pacific Council
 1137 for Energy and Mineral Resources ~~Earth Science Series, Volume 2. Houston, Texas.~~
 1138 [488 p.](#)
- 1139

- 1140 Scholl DW, Herzer RH 1994. Geology and resource potential of the southern Tonga–
 1141 Lau region. In: Stevenson AJ, Herzer RH, Ballance PF eds. Geology and Submarine
 1142 Resources of the Tonga-Lau-Fiji Region. SOPAC Technical Bulletin 8, In: Stevenson
 1143 AJ, Herzer RH, Ballance PF eds. Geology and Submarine Resources of the Tonga-Lau-
 1144 Fiji Region. SOPAC Technical Bulletin 8. Suva, Fiji, South Pacific Applied Geoscience
 1145 Commission. Pp. 329–335.
 1146
 1147 ~~Schumacher R & Schmincke H-U 1995. Models for the origin of accretionary lapilli.~~
 1148 ~~Bulletin of Volcanology 56: 626–639.~~
 1149
 1150 Siebert L, Simkin T 2002–2014. Volcanoes of the World: an Illustrated Catalog of
 1151 Holocene Volcanoes and their Eruptions. Smithsonian Institution, Global Volcanism
 1152 Program Digital Information Series, GVP–3,
 1153 (<http://www.volcano.si.edu/world/> accessed 12th December 2014).
 1154
 1155 Sigurdsson H, Sparks RSJ, Carey SN, Huang TC 1980. Volcanogenic sedimentation in
 1156 the Lesser Antilles Arc. The Journal of Geology 88(5): 523–540.
 1157
 1158 ~~Smellie JL 1984. Accretionary lapilli and vesiculated pumice in the Ballantrae ophiolite~~
 1159 ~~complex: ash fall products of subaerial eruptions. Report of the British Geological~~
 1160 ~~Survey 84(1), Pp.36–40.~~
 1161
 1162 Sparks RSJ, Bursik MI, Carey SN, Gilbert JE, Glaze L, Sigurdsson, H, Woods AW
 1163 1997. Particle aggregation in plumes, In: Volcanic Plumes. England, John Wiley &
 1164 Sons, England, Pp. 431–462.
 1165
 1166 Stevenson AJ, Childs JR 1985. Single channel seismic and geopotential data collection
 1167 and processing. In: Scholl DW, Vallier TL eds. Geology and Offshore Resources of
 1168 Pacific Island Arcs–Tonga Region. Circum-Pacific Council for Energy and Mineral
 1169 Resources Earth Science Series 2, In: Scholl DW, Vallier TL eds. Geology and
 1170 Offshore Resources of Pacific Island Arcs–Tonga Region. Earth Science Series 2,
 1171 Houston, Texas, Circum-Pacific Council for Energy and Mineral Resources. Pp. 27–29.
 1172
 1173 Stevenson AJ, Herzer RH, Ballance PF 1994. Contributions to the marine and onland
 1174 geology and resource assessment Geology and submarine resources of the Tonga-Lau-
 1175 Fiji region. SOPAC Technical Bulletin 8. Suva, Fiji, South Pacific Applied Geoscience
 1176 Commission. Springer Verlag, Berlin. 350 p.
 1177
 1178 Tappin DR 1993. The Tonga Frontal Arc Basin. In: Ballance PF, ed. South Pacific
 1179 Sedimentary Basins. Sedimentary Basins of the World, 2. Elsevier. Pp. 157–176.
 1180
 1181 Tappin DR, Ballance PF 1994. Contributions to the sedimentary geology of 'Eua Island,
 1182 Kingdom of Tonga: reworking in an oceanic forearc. In: Stevenson AJ, Herzer RH,
 1183 Ballance PF eds. Geology and Submarine Resources of the Tonga-Lau-Fiji Region.
 1184 SOPAC Technical Bulletin 8, In: Stevenson AJ, Herzer RH, Ballance PF eds. Geology
 1185 and Submarine Resources of the Tonga-Lau-Fiji Region. SOPAC Technical Bulletin 8.
 1186 Suva, Fiji, South Pacific Applied Geoscience Commission. Pp.1–20.
 1187
 1188 Tappin DR, Herzer RH, Stevenson AJ 1994. Structure and history of an oceanic
 1189 forearc- The Tonga Ridge - 22° to 26° south. In: Stevenson AJ, Herzer RH, Ballance PF
 1190 eds. Geology and Submarine Resources of the Tonga-Lau-Fiji Region. SOPAC

Formatted: Font color: Red

- 1191 [Technical Bulletin 8, In: Stevenson AJ, Herzer RH, Ballance PF eds. *Geology and*](#)
 1192 [Submarine Resources of the Tonga-Lau-Fiji Region. SOPAC Technical Bulletin 8.](#)
 1193 [Suva, Fiji, South Pacific Applied Geoscience Commission. Pp. 81–99+20.](#)
 1194
- 1195 Taylor B, Zellmer K, Martinez F, Goodliffe A 1996. Sea-floor spreading in the Lau
 1196 back-arc basin. *Earth and Planetary Science Letters* 144: 35–40.
 1197
- 1198 [Trofimovs J, Amy L, Boudon G et al. 2006. Submarine pyroclastic deposits formed at](#)
 1199 [the Soufriere Hills Volcano, Montserrat \(1995–2003\): what happens when pyroclastic](#)
 1200 [flows enter the ocean? *Geology*, 34: 549–552.](#)
 1201
- 1202 [Trofimovs J, Sparks, RSJ, Talling, PJ 2008. Anatomy of a submarine pyroclastic flow](#)
 1203 [and associated turbidity current: July 2003 dome collapse, Soufriere Hills volcano,](#)
 1204 [Montserrat, West Indies. *Sedimentology* 55: 617–634](#)
 1205
- 1206 Twiss RJ, Moores EM 2007. *Structural Geology*. New York, Freeman. 736 p.
 1207
- 1208 [Ui, T 1973. Exceptionally far-reaching, thin pyroclastic flow in Southern Kyushu,](#)
 1209 [Japan. *Bulletin of the Volcanological Society of Japan*. 2 \(18\): 153–168.](#)
 1210
- 1211 [Van Eaton AR, Herzog M, Wilson CNJ, McGregor J 2012 a\). Ascent dynamics of large](#)
 1212 [phreatomagmatic eruption clouds: The role of microphysics. *Journal of Geophysical*](#)
 1213 [Research - Solid Earth](#) 117(B3). doi:10.1029/2011JB008892.
 1214
- 1215 [Van Eaton AR, Muirhead JD, Wilson CNJ, Cimarelli C 2012 b\). Growth of ash](#)
 1216 [aggregates in the presence of liquid water and ice: an experimental approach. *Bulletin*](#)
 1217 [of *Volcanology* 74\(9\): 1963–1984.](#)
 1218
- 1219 Van Eaton AR, Wilson CNJ 2013. The nature, origins and distribution of ash
 1220 aggregates in a large-scale wet eruption deposit: Oruanui, New Zealand. *Journal of*
 1221 *Volcanology and Geothermal Research* 250: 129–154.
 1222
- 1223 [Walker GPL, Wilson L, Howell ELG 1971. Explosive Volcanic Eruptions I: The Rate](#)
 1224 [of Fall of Pyroclasts. *Geophysical Journal of the Royal Astronomical Society* 22: 377-](#)
 1225 [383](#)
 1226
- 1227 [Walker GPL \(1981\) Plinian eruptions and their products. *Bulletin of Volcanology* 144:](#)
 1228 [223-240.](#)
 1229
- 1230 White JDL, Smellie JL, Clague DA 2003. Introduction: A deductive outline and
 1231 overview of subaqueous explosive volcanism. *Geophysical Monograph Series, Volume*
 1232 *140 - Explosive Subaqueous Volcanism*, Pp.1–14.
 1233
- 1234 Wiesner MG, Wang Y, Zheng L 1995. Fallout of volcanic ash to the deep South China
 1235 Sea induced by the 1991 eruption of Mount Pinatubo. *Geology* 23: 885–888.
 1236
- 1237 [Woodhall D 1985. Geology of the Lau Ridge. In: Scholl DW, Vallier TL eds. *Geology*](#)
 1238 [and Offshore Resources of Pacific Island Arcs–Tonga Region. Circum Pacific Council](#)
 1239 [for Energy and Mineral Resources Earth Science Series 2, In: Scholl DW, Vallier TL](#)
 1240 [eds. *Geology and Offshore Resources of Pacific Island Arcs–Tonga Region. Earth*](#)

Formatted: Font color: Black

Formatted: Font color: Black

Formatted: Font color: Black

Formatted: Spanish (International Sort)

Formatted: Spanish (International Sort)

Formatted: Spanish (International Sort)

Formatted: Font color: Red

Formatted: Font color: Black

Formatted: Font color: Black

Formatted: Font color: Black

- 1241 | [Science Series 2. Houston, Texas, Circum-Pacific Council for Energy and Mineral](#)
1242 | [Resources](#). Pp. 351–378.
1243 |
1244 | ~~Wright IC 1996. Volcaniclastic processes on modern submarine arc stratovolcanoes:~~
1245 | ~~side-scan and photographic evidence from the Rumble IV and V volcanoes, southern~~
1246 | ~~Kermadec Arc (SW Pacific). Marine Geology 136: 21–39.~~
1247 |
1248 | Wright IC, Gamble JA 1999. Southern Kermadec submarine caldera arc volcanoes (SW
1249 | Pacific): caldera formation by effusion and pyroclastic eruption. Marine Geology 161:
1250 | 207–227.
1251 |
1252 | ~~Yamamoto T, Takada A, Ishizuka Y, Miyaji N, Tajima Y 2005 Basaltic pyroclastic~~
1253 | ~~flows of Fuji volcano, Japan: characteristics of the deposits and their origin. Bulletin of~~
1254 | ~~Volcanology 67, 622–633.~~
1255 |

Event	DRE (km^3)	Largest tephra (mm)	Distance from source (km)	Maximum distance (km)
Krakatoa	12	"small stone"	65	80
Kos Plateau Tuff				
Unit D	40	50	35	>30
Unit E	30	200	35	>60
Koya Tuff	1			>40

List of Tables

1258

1259

Table 1 Values for U_t , vertical terminal velocity at height, for particles of diameter 16 mm and density of 1500 kg m^{-3} , after Pfeiffer et al. (2005).

1262

1263

Table 24 — Dispersal of larger tephra by pyroclastic density currents travelling over the ocean surface (Carey et al. 1996, ~~from~~ Allen & Cas (2001), Carey et al. (1996) Maeno & Taniguchi 2007, Ui 1973) — DRE = dense rock equivalent. ~~Maximum distance = maximum dispersal distance estimated for the event.~~

1268

1269

Height (km)	Sea level	10	15	20	26
U_t (m sec ⁻¹)	17	27	48	50	100

1270

1271

List of Figures

1272

Table 2—Values for U_t , vertical terminal velocity at height, for particles of diameter

1273

16 mm, density of 1500 kg m⁻³ and F (sphericity) = 0.43, from Pfeiffer et al. (2005).

1274

List of Figures

Figure 1. — The position of the Lau Basin on the north end of the Tonga-Kermadec-Hikurangi trend and the study area. The Tonga frontal arc basin sediments (shaded) are broadly coincident with the 2000 meter isobath, after Tappin (1993). **Figure 1 Regional setting.** **A.** The position of 'Eua and Nomuka on the Tonga Ridge, and Vatoa and Ono-i-Lau on the Lau Ridge. The Tonga frontal arc basin sediments (shaded) are broadly coincident with the 2000 meter isobath, after Tappin (1993). **B.** The Tonga Ridge platform, highlighted by the 1000 meter isobath, with the currently active back-arc Tofua volcanic chain, with block margins after Tappin et al. (1994), Scholl & Vallier (1985), Austin et al. (1989).

Figure 2 Accretionary lapilli from 'Eua. **A.** Layered accretionary lapilli with coarse ash infill. **B.** Layered accretionary lapilli, some cored, with coarse ash infill. **C.** Rimmed accretionary lapillus. **D.** Rare cross-bed in host volcanoclastics.
—Base map from GeoMapApp, <http://www.geomapapp.org>.

Figure 2. — Synthesis of data centred on the Lau Basin, after Taylor et al. (1996), with c. 20° easterly rotation of the Tonga Ridge (solid black lines) after Sager et al. (1994). **Figure 3** Lau Basin tectonics. **A.** Synthesis of data centred on the Lau Basin, after Taylor et al. (1996), with c. 20° easterly rotation of the Tonga Ridge (solid black lines) after Sager et al. (1994). **B.** Outline reconstruction of the ancestral Lau/Tonga ridge, pre-Lau Basin formation, just after splitting commenced, with bathymetric contours. **C.** Schematic section of the Lau Ridge, Lau Basin and Tonga Ridge with ODP sites, at c. 1.5-1.0 Ma, after Clift et al. (1995), modified to reflect the work of Parson & Wright (1996).

base map from GeoMapApp, <http://www.geomapapp.org>. Extended legend as follows:

834 Late Miocene	ODP site and age at base of well
Lighter areas (2A)	Areas where palaeomagnetic data correlates with known age ranges, none older than the Gauss isochron (<3.3 Ma)
1, 2, 2A	Subdivisions of isochrons
J	Jaramillo isochron
CLSC/ELSC	Central Lau Spreading Centre/East Lau Spreading Centre
ETZ/NWSLC/MTJ	Extensional Transform Zone/NW Lau Spreading Centre/Mangatolo Triple Junction
Dashed line	West of this line, is the "extended ancestral arc crust"
Dotted line	Eastern edge of Lau Ridge/western edge of Tonga Ridge

Figure 3. — Schematic section of the Lau Ridge, Lau Basin and Tonga Ridge with ODP sites, at c. 1.5-1.0 Ma, after Clift et al. (1995), modified to reflect the work of Parson and Wright (1996).

Figure 4. — The Tonga Ridge platform, highlighted by the 1000 meter isobath, with the currently active back arc Tofua volcanic chain, with block margins and selected track lines, after Tappin et al. (1994), Scholl and Vallier (1985), Austin et al. (1989), Lehner et al. (1983).

Formatted: Font: Not Bold

Formatted: Font: Bold

Formatted: Font: Bold

Formatted: Font: Not Bold

Formatted: Widow/Orphan control, Adjust space between Latin and Asian text, Adjust space between Asian text and numbers

1326
1327
1328
1329
1330
1331
1332
1333
1334
1335
1336
1337
1338
1339
1340
1341
1342
1343
1344
1345
1346
1347
1348
1349

Figure 5. — Fiji and the Lau islands, after Cole et al. (1985), bathymetric contour interval 2000 meters. The inset box outlines the Lau Islands whose geology was reported by Woodhall (1985), the most southerly of which is Ono-i-Lau.

Figure 6. — **A**, 'Eua: Mn-coated accretionary lapillus. **B**, 'Eua: rare large lithic clast (14 mm) in host volcanoclastics. **C**, 'Eua: rimmed accretionary lapillus. **D**, 'Eua, rare cross-bed in host volcanoclastics. Ruler scale is cm/mm.

Figure 7. — Outline reconstruction of the ancestral Lau/Tonga ridge, pre-Lau Basin formation, just after splitting commenced.

Figure 8. — Discontinuity of trends across the boundary between Blocks A, B and T-E.

Figure 4. — Discontinuity of trends across the boundary between tectonic Blocks A, B and T-E. Trend of gravity and arc basement highs on Blocks A and B is superimposed on residual magnetic anomaly data from Stevenson & Childs (1985), determined by subtracting the 1975 International Geomagnetic Reference Field (IAGA, 1976) from the observed total field measurements. Trend of basement highs on Block T-E is superimposed on total magnetic intensity data from Gatliff et al. (1994).

Figure 9. — Left: basement trends and faults on Blocks A, T-E and N, after Cunningham & Anson (1985). Right: rotation effect of strike-slip faulting on arcuate faults, accommodated by strike-slip faulting on a curved fault "hinge", after Lamb (2011).

Formatted: Pattern: Clear (White)